



# Optimizing the maintenance threshold in presence of shocks: A numerical framework for systems with non-monotonic degradation

Bahareh Tajjani<sup>a,\*</sup>, Jørn Vatn<sup>a</sup>, Masoud Naseri<sup>b</sup>

<sup>a</sup> Department of Mechanical and Industrial Engineering, Norwegian University of Science & Technology (NTNU), Trondheim 7491, Norway

<sup>b</sup> Department of Technology and Safety, UiT The Arctic University of Norway, Tromsø 9037, Norway

## ARTICLE INFO

### Keywords:

Maintenance threshold optimization  
Stochastic shocks  
Lead time  
Wiener process

## ABSTRACT

Shocks have attracted considerable interest in reliability and maintenance engineering because of their impact on vulnerable systems. Most industrial systems suffer from both internal degradation caused by fatigue and wear-out, and external shocks that often occur randomly due to harsh weather conditions, overloading, etc. Developing maintenance optimization models without taking these stochastic shocks into account is often ineffective. This paper develops a model to optimize the maintenance alarm threshold for a single-component continuously monitored system which is exposed to both fatal and non-fatal shocks in the presence of lead time for hard time maintenance. The shocks occur randomly according to a homogeneous Poisson process during the whole degradation process and have a stochastic impact on the degradation level, while the system resistance to shocks decreases as the system approaches failure. We propose a new numerical maintenance optimization model to find the solution without Monte-Carlo simulation and the model is compared to the Wiener process. A numerical example and a real-time experimental case study on roller bearings are used to demonstrate the effectiveness of the model. The results show that the model is capable of improving maintenance decision-making in terms of failure probability and risk perspective.

## 1. Introduction

Shock models have been the focus of many researchers during the past few decades due to their extensive applications within operational research, maintenance modeling, and reliability theory. The failure of many engineering complex systems arises not only from internal gradual degradation such as wear-out, fatigue, and aging, but also from external shocks, which are mostly due to external causes, for instance overload, vibrations, or harsh environmental conditions [19,36]. Recently, various studies have focused on reliability analysis and maintenance policy optimization of systems exposed to competing failures. Gradual degradation of such systems are usually modelled by general path models, pure data-driven machine learning algorithms, and stochastic processes [20]. On the other hand, external shock models are divided into five categories, namely cumulative, run, delta, extreme, and mixed shock models [39]. Shocks due to external environment may lead to unexpected system failures and huge economic losses. Thus, it is very important to develop an effective and efficient maintenance plan for systems considering both gradual degradation and external shocks [19].

### 1.1. Literature review

#### 1.1.1. Systems with gradual degradation

Traditionally, most researchers focused on optimization of condition-based maintenance (CBM) policies considering the system's gradual degradation without taking external shocks into account. For instance, Wang et al. [35] modelled the natural degradation process using a monotonic non-decreasing Gamma process and proposed a CBM framework for continuously monitored systems, where the scheduling threshold for lead time to request the maintenance is integrated with maintenance and failure thresholds. Wang et al. [40] proposed a system replacement policy based on condition monitoring information. The system failure is induced by only natural degradation and is modelled by a non-monotonic Wiener process. Grall, Bérenguer and Dieulle [15] developed an analytical model to minimize the long-run expected cost per unit time following a condition-based inspection/replacement policy for a stochastically deteriorating system, whose states are assumed to be perfectly known by means of inspections. Bérenguer et al. [2] proposed a maintenance policy for a system with continuous states, in which its stochastic degradation is modelled by a Gamma process. The alarm threshold was optimized by minimizing the asymptotic

\* Corresponding author.

E-mail address: [bahareh.tajjani@ntnu.no](mailto:bahareh.tajjani@ntnu.no) (B. Tajjani).

<https://doi.org/10.1016/j.ress.2024.110039>

Received 20 July 2023; Received in revised form 20 February 2024; Accepted 23 February 2024

Available online 24 February 2024

0951-8320/© 2024 The Authors. Published by Elsevier Ltd. This is an open access article under the CC BY license (<http://creativecommons.org/licenses/by/4.0/>).

Notations			
$C_R$	Cost of replacement per unit time	$B(\bullet)$	The standard Brownian motion
$C_F$	Cost of failure per unit time	$\eta$	Drift parameter of Wiener process
$C_U$	Cost of downtime per unit time	$\sigma_B$	Diffusion parameter of Wiener process
$T_M$	The time when maintenance alarm is triggered and mobilization for maintenance is started (first hitting time of the maintenance threshold $M$ )	$\nu$	Mean parameter of Inverse Gaussian (IG) distribution
$T_C$	The time when renewal is completed	$\kappa$	Shape parameter of Inverse Gaussian (IG) distribution
$T_F$	Failure time (first hitting time of the failure threshold $L$ )	$\rho$	Intensity factor of homogeneous Poisson process
$M$	Maintenance threshold	$s$	Stochastic magnitude of a shock
$L$	Deterministic failure threshold	$u(s)$	The probability density function of the shock's magnitude $s$
$DT$	Downtime	$\alpha$	Shape parameter of Gamma distribution
$E(DT M)$	Expected downtime as a function of the maintenance threshold $M$	$\lambda$	Scale parameter of Gamma distribution
$T_L$	Lead time	$f_Y^b(\bullet)$	The probability density function (PDF) of degradation level $y$ in Case 1-I
$MTTM$	Mean time to reach the maintenance threshold $M$	$f_Y^a(\bullet)$	The probability density function (PDF) of degradation level $y$ in Case 1-II
$M^*$	Optimal maintenance threshold	$q_Y^b(\bullet)$	The probability density function (PDF) of degradation level $y$ in Case 2-I
$C(M^*)$	Expected cost at $M^*$	$q_Y^a(\bullet)$	The probability density function (PDF) of degradation level $y$ in Case 2-II
$y(t)$	System degradation level at time $t$	$w_Y^b(\bullet)$	Final PDF of degradation level $y$ when $y$ is below maintenance threshold $M$ , Case 2-I
$a_{\Delta t}$	Degradation increment from time $t$ to time $t + \Delta t$	$w_Y^a(\bullet)$	Final PDF of degradation level $y$ when $y$ is above maintenance threshold $M$ , Case 2-II
$g(a)$	The probability density function of the random degradation increment $a$		

unavailability of the system assuming a deterministic lead time. Jiang [20] proposed a cost model for a system with a monotonically increasing degradation process to optimize the maintenance alarm threshold and first inspection time. General path model, increment process model, and a condition-based degradation model are presented to solve the problem. Elwany et al. [12] developed a replacement decision model to find the optimal replacement time for continuously monitored systems which follow a stochastic exponential model. As the first step, the stochastic degradation model is used to update the predictive distribution of the component's degradation signals by means of a Bayesian approach, while the second step focused on modeling the replacement decision using a Markov decision process.

However, as previously mentioned, the optimal CBM policies in these studies were developed by considering only gradual deterioration of systems, while the impact of external shocks on the system degradation and maintenance decision-making was overlooked. In reality, a large variety of engineering complex systems such as offshore wind turbines are not only subject to degradation but also exposed to external shocks caused by harsh marine environments, icing, waves, and earthquakes [3].

### 1.1.2. Systems with gradual degradation and shocks

Recently, models that simultaneously consider degradation processes and shocks have been proposed for reliability and maintenance modeling of systems with discrete states and continuously monitored systems. In some literature, they are called degradation-threshold-shock (DTS) models [5].

With regard to systems with discrete states, researchers have focused on developing optimal maintenance policies using discrete models such as a Markov chain process. For instance, Byon, Ntamo and Ding [4] derived an optimal preventive maintenance policy for wind turbines by minimizing the long-run expected cost, where the authors use a Markov decision process to formulate the problem. Sarada and Shenbagam [31] also presented a preventive maintenance replacement strategy for a deteriorating repairable system with stochastic lead time via a phase-type quasi-renewal process, which is a discrete-time stochastic process to model events that happen at random times.

Gan, Hu and Coit [13] proposed an optimal maintenance policy where a multi-state system is exposed to changing environment states,

where the system and the environment can influence each other. The authors use a Markov decision process to formulate the problem and find the optimal maintenance action at the decision time (i.e., do nothing, replacement, imperfect repairs). Wang et al. [37] focused on a balanced system with multi-state components that work during multiple sequential stages. The system becomes unbalanced when one of the components fails, and the component's degradation characteristics vary based on external environments or working loads. A Markov decision process is used to model the system operation and find the optimal joint strategies.

Yang et al. [41] also proposed a preventive maintenance policy for a single-component system whose failure is due to gradual deterioration and fatal shocks. The gradual deterioration is composed of two normal and defective stages, and it is modelled by the delay-time concept. The occurrence of external shocks is modelled by a non-homogeneous Poisson process (NHPP) and their objective is to find the preventive maintenance interval, inspection time, and the number of inspections. However, assuming that external shocks arrive at random times according to a NHPP is not aligned with the characteristics of the shocks. In other words, although the system is more vulnerable to shocks as it approaches failure, the intensity rate or the shocks' rate of occurrence is not time dependent. This means that the shocks can occur randomly at any point in time, irrespective of the system's age or condition. Thus, to capture the random shocks, which are unpredictable events caused by external factors, a homogeneous Poisson process (HPP) is a more suitable modeling approach. Lin, Li and Zio [25] also analyzed the reliability of a system subject to dependent degradation process and random shocks using two methods of Monte-Carlo simulation (MCS) and finite-volume methods. The Piecewise Markov process was used to model the degradation and its dependencies with the random shocks. In addition, Liang, Peng and Li [23] proposed a multi-state degradation model for nuclear piping systems that are subject to dynamic environment condition, fatigue degradation, and random shocks, where the evolutions of fatigue degradation and dynamic environment are described and modelled by Markov-based processes. A recent study on systems with shocks and degradation was carried out by Wang and Chen [38], who proposed a condition-based imperfect maintenance policy using piecewise deterministic Markov process considering a deterministic maintenance delay or lead time.

In the aforementioned studies, the reliability and maintenance models are mostly suitable for systems with discrete states. These models rely on discrete modeling techniques such as the Markov process to represent degradation, shocks and, in some cases, the dependencies between them. Thus, developing maintenance models for continuously monitored systems exposed to random shocks still requires further investigation.

When it comes to the maintenance models for continuously monitored systems with competing failures, several researchers have proposed various approaches for the optimization of maintenance alarm threshold, inspection intervals, inspection delay, and condition-based policies. As an example, Zhao et al. [46] proposed an analytical solution for an optimal condition-based maintenance policy, where the failures were induced by random shocks and deterioration. However, their research work is different from ours in various aspects. First, the random shocks are modelled according to a NHPP and are assumed to be fatal (i.e., shocks that lead to system failure immediately), while non-fatal shocks (i.e., shocks that have stochastic impact on the degradation level, but does not cause system failure) were not considered. Second, the system degradation is modelled by a monotonic Gamma process, and thus the proposed algorithm can not be extended to systems with non-monotonic degradation behavior.

In Castro, Caballé and Pérez [6], a condition-based maintenance framework of a system subject to multiple sources of failures was developed. The degradation and shocks were modelled by a stochastic Gamma process and a NHPP, respectively. The shocks could arrive to the system at random times and the system state was checked at regular inspection times. The focus was to find the optimal inspection time while the inspection delay or lead time was assumed to be negligible in their work. Deloux, Castanier and Bérenguer [8] also worked on a predictive maintenance policy for a gradually deteriorating system subject to stress, while they used a different modeling approach than our model based on their application context. They modelled the gradual increasing deterioration by a phase-type distribution, where the degradation increment over one fixed time unit is an exponential distribution. Phase-type distribution is a classical and widely used way of modeling the cumulative wear, crack growth, and fatigue.

Yousefi et al. [42] developed a maintenance optimization model for multi-component systems to determine optimal condition-based failure thresholds and inspection intervals, where each component was exposed to both degradation and shock loads. However, the authors did not consider the impact of lead time on the optimal failure threshold. The components degradation were modelled by a Gamma process and the random shocks followed a Poisson process. Li and Pham [22] proposed a condition-based maintenance model for a system subject to two degradation processes (i.e., random coefficient degradation path and randomized logistic degradation path function) and random shocks, which are modelled according to a Poisson process. The expected maintenance cost rate function was derived to find the optimal preventive maintenance threshold and the inspection time based on a geometric sequence. The system state in the authors' study could only be revealed after an inspection. Pedersen, Liu and Vatn [29] developed a condition-based maintenance policy for a two-component system that is exposed to continuous degradation and hard failure. They assumed that the degradation of one component is divided into a stable phase and a deterioration phase, and that the other component is not subject to aging, but it is subject to hard failure, which is the system's sudden breakdown. The characteristics of their system of concern and their modeling framework are different from ours. The system, exposed to continuous degradation, remains healthy until the arrival of a shock that introduces a potential failure, similar to the PF model. The authors focused on finding the imperfect repair threshold and preventive renewal time by minimizing the long-run expected cost rate. In our paper, we consider the probability of a shock occurring in each time interval, taking into account possible scenarios that may arise as a result.

Additionally, Liang, Yang and Peng [24] developed a reliability

model for systems subject to mutually dependent degradation process and random shocks, where the degradation is modelled by a time-homogeneous stochastic process on a continuous state space, in particular a Gamma process, and the random shocks are modelled by a time-homogeneous semi-Markov process on a finite state space. Zhang et al. [43] also proposed a degradation-threshold-shock model for a system operating under dynamic environment conditions which affect the system degradation and shocks. A Gamma process is used to model the system degradation, and the environment condition is modelled via a continuous-time Markov chain.

In the majority of the above literatures, a Gamma process for continuously monitored systems and a Markov process for systems with discrete states have been used to model the baseline degradation. However, Gamma processes are applicable for systems that degrade monotonically.

Among several researchers who worked with a Wiener-based process as the baseline degradation model, Liu et al. [27] used a non-linear Wiener process to develop a maintenance model for mission-oriented systems that are affected by gradual degradation and shocks. However, the method in Liu et al. [27] is not a fully numerical approach as the authors rely on MCS to derive the long-run cost rate. Hao and Yasng [16] also used a non-linear Wiener process to model the air leakage of gas insulated transmission and considered the random degradation initiation time and degradation-shock dependence simultaneously. Sun et al. [32] also proposed a general reliability model for a system with multiple degradation processes, where fatal and non-fatal shocks were incorporated in the model and a time-varying copula method was used to consider the dependency between the shocks and the internal degradation. However, the lead time impact was not considered in their work, and their modeling frameworks were different to ours with respect to both shocks and baseline degradation. Furthermore, Duan et al. [10] proposed a deterioration-integrated failure model where the degradation data, failure events, and environment conditions are integrated in the model. The authors use a random-effect Wiener process that has a stochastic drift parameter accounting for the stochastic impact of environment, and a proportional hazards (pH) model to incorporate multiple sources of information through covariates. However, their model does not account for lead time or maintenance delay.

As previously mentioned, despite the importance of lead time in maintenance and reliability models, it has not been thoroughly studied or integrated into the maintenance models before. Many have considered instantaneous maintenance, meaning that, when a maintenance decision has been made, the system can be restored to the working state immediately. However, this is difficult to achieve in practice. A long lead time can infer several challenges, such as the unavailability of critical spare parts to carry out maintenance and huge production loss [14,31,34]. As an example, in subsea production systems, maintenance crew may require several months to finalize maintenance tasks, depending on the weather condition and resource mobilizations [44]. Neglecting lead time can lead to an underestimation of the failure risk of the system, leading to a suboptimal maintenance policy. When maintenance is finalized while accounting for lead time, the decision-maker might become more conservative when scheduling and developing future maintenance strategies. The lead time could potentially affect the decision-making process to prioritize safety or avoid potential issues that may arise as a result of lead time.

In our paper, we consider the system failure probability in lead time in our numerical framework to optimize the maintenance alarm threshold for systems with non-monotonic degradation behavior without resorting to MCS. The system baseline degradation is a linear Wiener process, while the incorporated lead time benefits decision-makers to have a more realistic and risk-informed decision-making.

## 1.2. Contributions

To the best of our knowledge, optimizing the maintenance threshold

for continuously monitored systems, subject to random shocks with different stochastic magnitudes, while taking lead time into account, is rare in existing literature. There are a few researchers who have focused on the reliability and maintenance of such systems, but they use a Gamma process which is suitable for systems with monotonically increasing degradation process [9,46], or they use the Markov chain approach which only applies to systems with discrete states [21]. Some researchers have worked with a non-linear Wiener process for modeling the gradual degradation and shocks; however, they resort to MCS for deriving the optimization function, or they do not consider the impact of lead time or maintenance delay in their models [10,11].

The main methodological contribution is to propose a novel numerical routine that efficiently finds the optimal maintenance threshold for systems that are subject to competing failures without relying on MCS. We have chosen a Wiener process to model the system baseline degradation due to its non-monotonic degradation property that offers advantages over the Gamma process and aligns more closely with the characteristics of real-life applications. We propose the numerical solution in two cases: in Case 1, the system is exposed to only gradual degradation and, in Case 2, we extend the model to incorporate random shocks. The shocks are not only fatal, which are often addressed by previous literature, but they can be of different severity or magnitudes and, thus, increase the degradation level by a random extent. Shocks with low severity (i.e., shocks with small magnitudes) can cause only accumulated damage; however, this does not lead to direct failure, while shocks with high severity (i.e., shocks with large magnitudes) can lead to a system failure directly. The purpose of the numerical algorithm is to find the optimal maintenance threshold by minimizing the total expected cost.

Additionally, lead time was integrated in the model. During this period, the system will still suffer from gradual degradation and random shocks while waiting for maintenance. Thus, the system failure probability was considered during the lead time. It was demonstrated that the integration of lead time in maintenance and reliability models can improve maintenance decision-making, whereas neglecting lead time results in an underestimation of the failure probability and delayed maintenance.

Moreover, the impact of shock detection threshold on the objective function (i.e., total expected cost) was analyzed using a number of simulated datasets to figure out which detection threshold can correctly capture the real shocks in the data. It was presented that a high detection threshold underestimates the total expected cost and leads to suboptimal maintenance decisions, while lower thresholds can capture a large number of shocks, providing more accurate results.

We developed a Monte-Carlo algorithm for simulation of stochastic processes, including the system degradation and shocks, to verify the correctness of the proposed model. The effectiveness of the proposed model was demonstrated by applying the model on a numerical example and a laboratory dataset collected from experiments on rotating bearings. The results of this paper can further contribute to replacement and maintenance decision-making to improve system availability and reduce production downtime.

The rest of this paper is structured as follows. Section 2 presents the model description. Section 3 and Section 4 provide the results and discussion, and Section 5 describes the conclusions and further work.

## 2. Model description

Consider a single-unit system with a stochastic degradation process  $y(t)$  and external shocks. The degradation process is described by a non-monotonic linear Wiener process (i.e.,  $y(t) \sim W(\eta t, \sigma_B \sqrt{t})$ ). The failure time  $t_F$  is when the degradation level  $y(t)$  hits a given known failure threshold  $L$ . The external stochastic shocks arrive to the system according to a homogeneous Poisson process with a constant intensity factor  $\rho$ . The random shocks are classified into two categories: fatal

shocks and non-fatal shocks. Fatal shocks are the ones that have a large impact on the degradation process, which cause the degradation level to surpass the failure threshold  $L$  instantaneously. Non-fatal shocks are the ones that increase the degradation level by a stochastic magnitude, while the degradation level  $y(t)$  after the shock still remains below the failure threshold  $L$ .

In a time interval  $\Delta t$ , there is a probability  $\rho \Delta t$  that a shock occurs. The probability that the system experiences failure by a fatal shock increases as the system approaches the failure threshold. In other words, the system's resistance to a fatal shock decreases gradually through the system's lifetime due to the progressive deterioration of the system's health condition. The maintenance alarm is triggered and the mobilization for maintenance is started when the degradation level  $y(t)$  hits the maintenance threshold  $M$  at time  $t_M$ . It is assumed that there is a constant lead time  $T_L$  from the time that the maintenance alarm is triggered (i.e.,  $t_M$ ) until the renewal process is completed (i.e.,  $t_C$ ). It is assumed that at time  $t_C$ , the system will be renewed and revert back to "as good as new" condition. The constant lead time is valid for some systems that have a constant time to complete a maintenance activity. For instance, a battery replacement in different equipment such as a gas detector, a smoke detector, or a portable device can be a maintenance task with constant lead time. The system may fail due to gradual degradation or external stochastic shocks during the lead time  $T_L$  (i.e.,  $t_F < t_C$ ) and experience a period of downtime  $DT$  (i.e., alternative a in Fig. 1). On the other hand, the system may survive until the maintenance time  $t_C$  where it will be preventively maintained with no downtime (i.e., alternative b in Fig. 1). Fig. 1 is an illustrative picture of a sample degradation path with the two alternatives. For the sake of clarity, the shocks are not shown in Fig. 1; however, they will be illustrated later in detail.

The goal is to find the maintenance threshold  $M$  that minimizes the long-run cost rate. Eq. (1) presents the long-run cost rate, which is the expected renewal cycle cost divided by the expected renewal cycle length.

$$C_\infty(M) = \lim_{t \rightarrow \infty} \frac{C(t; M)}{t} = \frac{E[C(t_C|M)]}{E[t_C|M]} \quad (1)$$

where  $E[t_C|M]$  is the expected length of a renewal cycle and  $E[C(t_C|M)]$  is the expected non-discounted cost within a renewal cycle as a function of maintenance threshold  $M$  [30].

Based on Eq. (1), in our model, the expected cost rate per renewal cycle as a function of a maintenance threshold  $M$  is as follows:

$$C_\infty(M) = \frac{C_R + C_F \cdot \Pr(t_F(t_C|M)) + C_U \cdot E[DT|M]}{MTTM + T_L} \quad \text{for } M \in [0, L] \quad (2)$$

where  $C_\infty(M)$  is the expected long-run cost, which is a function of maintenance threshold  $M$ ,  $C_R$  is the replacement cost,  $C_F$  is the cost of failure, and  $C_U$  is the cost of downtime per unit of time.  $\Pr(t_F(t_C|M))$  is the probability of failure in lead time and  $E[DT|M]$  is defined as the expected downtime  $E[DT]$  as a function of maintenance threshold  $M$ . Mean time to maintenance  $MTTM$  is the expected time for the maintenance alarm to be triggered in order to mobilize for maintenance. Alternatively, it can be expressed as the mean time to reach the maintenance threshold  $M$  as a function of  $M$  (i.e.,  $MTTM = E[t_M|M]$ ).

According to Eq. (3), assuming that there is only one maintenance threshold  $M$ , the objective is to select the optimal maintenance threshold  $M^*$  to minimize the expected cost per unit time in a long run.

$$M^* = \arg_M \min[C_\infty(M)] \quad (3)$$

In the following sections, we propose a numerical framework for two different cases. Case 1 represents a Wiener process, where the gradual degradation occurs primarily due to aging and the model does not consider external shocks. In Case 2, we consider the influence of external shocks on the deterioration process.

In both cases, to calculate the expected cost rate as a function of maintenance threshold  $M$ , the numerical framework is divided into two

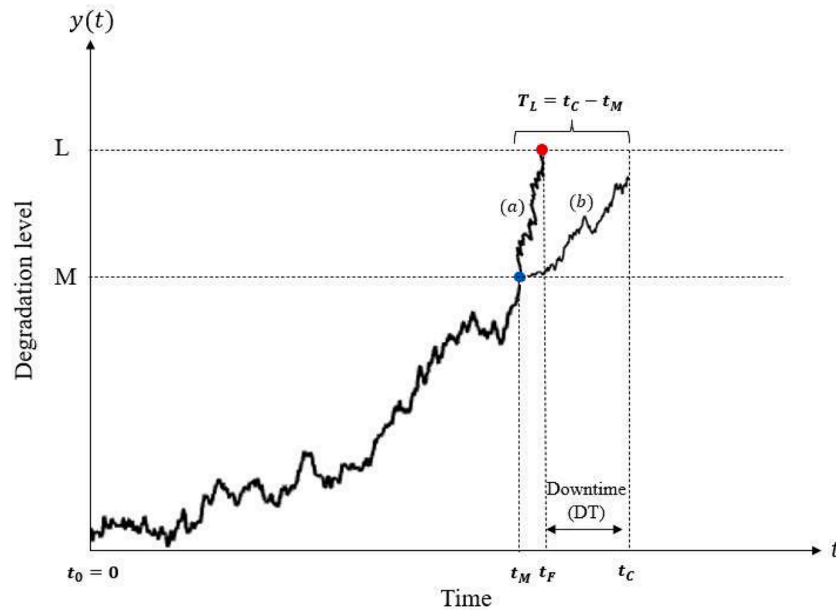


Fig. 1. Illustration of a sample degradation path.

interconnected parts. I) The first part covers the period from the system's initial operation at time zero (i.e.,  $y(t_0) = 0$ ) until it reaches the maintenance threshold (i.e.,  $y(t_M) = M$ ), triggering maintenance alarm, where MTTM is calculated as a result of this part. II) The second part focuses on the period when the degradation level is above maintenance threshold M, where  $\Pr(t_F|t_C|M)$  and  $E[DT|M]$  are calculated as outcomes of the second part.

• **Case 1: Modeling – Gradual degradation**

Case 1-I) When degradation level  $y$  is below maintenance threshold  $M$  (i.e.,  $y(t) \in [0, M]$ )

Case 1-II) When degradation level  $y$  is above maintenance threshold  $M$  (i.e.,  $y(t) \in [M, L]$ )

• **Case 2: Modeling – Gradual degradation and external shocks**

Case 2-I) When degradation level  $y$  is below maintenance threshold  $M$  (i.e.,  $y(t) \in [0, M]$ ) Case 2-II) When degradation level  $y$  is above maintenance threshold  $M$  (i.e.,  $y(t) \in [M, L]$ )

In the numerical framework, the purpose is to calculate the probability density function (PDF) of the degradation level  $y$  at time  $t + \Delta t$  as a function of the PDF of  $y$  at time  $t$ . In Case 1-I and Case 1-II,  $f_Y^b(\cdot)$  and  $f_Y^a(\cdot)$ , and in Case 2-I and Case 2-II,  $q_Y^b(\cdot)$  and  $q_Y^a(\cdot)$  are used to represent the PDF of degradation level  $y$  when  $y$  is below and above the maintenance threshold  $M$  respectively.

There are two main assumptions in this model. First, once the degradation level  $y$  reaches the maintenance threshold  $M$ , the maintenance alarm is triggered and the degradation level  $y$  does not decrease below maintenance threshold  $M$  thereafter. Thus, in Cases 1-I and 2-I where  $y(t) \in [0, M]$ , we remove the probability that the system degradation level exceeds maintenance threshold  $M$  at time  $t$  before updating the PDF at time  $t + \Delta t$ . In Case 2-I, we introduce a vector  $\varphi_Y(\cdot)$  for  $y \geq M$  to cumulatively store the probability of system degradation level  $y$  over time  $t$ , which is necessary for subsequent computations in Case 2-II.

Second, failure occurs when the degradation level  $y$  reaches the failure threshold  $L$  for the first time and it does not return to below the failure threshold  $L$  afterwards. To hold this assumption, in Cases 1-II and 2-II where  $y(t) \in [M, L]$ , we first store the probability that the system

surpasses the failure threshold  $L$  at time  $t$  in a vector called  $m(t)$ , and then remove it before updating the PDF at time  $t + \Delta t$ .

The details of the numerical process for both cases are demonstrated below. In Case 1, the proposed numerical framework is compared with an analytical approach and, in Case 2, we compare it with MCS.

2.1. Case 1: Modeling-Gradual degradation

In Case 1, where the system is only exposed to gradual degradation followed by a Wiener process and the impact of shocks are excluded from the model, the degradation can be modelled analytically. This arises from the fact that the first hitting time (FHT) or the first time that the degradation level  $y(t)$  surpasses the predetermined failure threshold  $L$  is analytically known as Inverse Gaussian (IG) distribution. Thus, the optimization of the expected cost to find the optimal maintenance threshold  $M^*$  in this case is rather straightforward. However, since the model in Case 1 serves as a solid basis to build up the model in Case 2, we solve the model numerically, such that we can extend it later to incorporate additional features (i.e., stochastic external shocks) in order to enhance its performance for real-world scenarios.

2.1.1. Numerical approach

In a conventional Wiener process, the degradation process  $\{y(t); t \geq 0\}$  is usually formulated as follows:

$$y(t) = y_0 + \eta t + \sigma_B B(t) \tag{4}$$

where  $y_0$  is the initial degradation level of the concerned system,  $\eta$  is the drift coefficient capturing the rate of degradation,  $\sigma_B$  is the diffusion coefficient, and  $B(t)$  is a standard Brownian motion representing the stochastic dynamic of the degradation process [30,45]. The main properties of the Wiener process are listed as follows:

- Property 1: The starting point in the degradation process is known:  $\Pr(y(t_0 = 0) = 0) = 1$
- Property 2: Degradation increments are independent. For any  $0 \leq t_1 < t_2 < \dots < t_n < \infty$ ,  $y(t_2) - y(t_1), \dots, y(t_n) - y(t_{n-1})$  are independent.
- Property 3: Degradation increments are stationary and normally distributed.  $y(t) - y(e)$  has the same distribution as  $y(t - e)$ ,  $\forall e \leq t$ .

As stated before, in the numerical framework, the purpose is to calculate the PDF of the degradation level  $y$  at time  $t + \Delta t$  (i.e.,  $f_Y(y, t + \Delta t)$ ) as a function of the PDF of  $y$  at time  $t$  (i.e.,  $f_Y(y, t)$ ) for  $t \geq 0$ .

**Case 1-I) degradation level below maintenance threshold  $M$ .** As presented in Eq. (5), if the degradation level of a system at time  $t$  is denoted by  $y(t)$  for  $t \geq 0$ , there is a deterioration occurring in the system with a random quantity  $a$  in a time interval  $\Delta t$  from  $t$  to  $t + \Delta t$ . Due to the non-monotonic characteristic of the Wiener process, the deterioration quantity  $a_{\Delta t}$  (i.e., degradation increment) can have both a positive and negative value.

$$y(t + \Delta t) = y(t) + a_{\Delta t} \quad (5)$$

We assume that the time interval  $\Delta t$  is determined and, thus, we simplify the notation of  $a_{\Delta t}$  as  $a$ . Let  $g(a)$  be the PDF of the random degradation increment  $a$  from time  $t$  to  $t + \Delta t$ . According to Eq. (6), if the PDF of  $y$  at time  $t$  (i.e.,  $f_Y^b(y, t)$ ) is known, the PDF of  $y$  at time  $t + \Delta t$  (i.e.,  $f_Y^b(y, t + \Delta t)$ ) can be obtained using the law of total probability.

$$f_Y^b(y, t + \Delta t) = \int_{-\infty}^{\infty} f_Y^b(y - a, t) g(a) da \quad (6)$$

where  $a$  is the degradation increment from time  $t$  to  $t + \Delta t$  and  $f_Y^b(y - a, t)$  is the PDF of the degradation level  $y - a$  at time  $t$ . As presented in Eq. (7), according to the Wiener process, the PDF of the increments follows a normal distribution (property 3) (i.e.,  $g(a) \sim N(\mu, \sigma_B^2)$ ). Since it is assumed that the system fails when the deterioration level exceeds the predefined failure threshold  $L$ , Eq. (6) should be modified into Eq. (8).

$$g(a; \mu, \sigma_B^2) = \frac{1}{\sigma\sqrt{2\pi}} e^{-\frac{(a-\mu)^2}{2\sigma^2}} \quad (7)$$

$$f_Y^b(y, t + \Delta t) = \int_{y-L}^{\infty} f_Y^b(y - a, t) g(a) da \quad (8)$$

Fig. 2 is an illustration of the numerical process in Case 1-I when  $y(t) \in [0, M]$  along with a realization of a degradation process. It presents how the PDF of the degradation level  $y$  is updated iteratively over time throughout the degradation process. Since Case 1-I is specifically related to  $y(t) \in [0, M]$ , we did not illustrate the degradation level  $y$  beyond the

point where it reaches the maintenance threshold  $M$ . However, the propagation of PDF of  $y$  continues until  $t = k\Delta t$ .

As in the Wiener process, the starting point in the degradation process is known (property 1) (i.e.,  $y(t_0) = 0$ ), the deterioration level at the first time step is  $y(t = \Delta t) = y(t_0 = 0) + a$ . Thus, the initial PDF of  $y$  at the first time step  $\Delta t$  (i.e.,  $f_Y^b(y, t = \Delta t)$ ) in Fig. 2 is the same as the distribution of increments  $g(a)$  which is a Normal distribution presented in Eq. (7).

The initial PDF  $g(a)$  at time  $\Delta t$  (i.e.,  $f_Y^b(y, \Delta t)$ ) is then used as the starting point to update the PDF at the next time steps (i.e.,  $2\Delta t, 3\Delta t, \dots, n\Delta t$ ). In order to reduce the computational time, we stop the iteration process of updating the PDF of  $y$  at some time  $t$  where the probability of the system not exceeding the maintenance threshold  $M$  becomes zero for

the first time (i.e.,  $\int_0^M f_Y^b(y, t) dy = 0$ ). For instance, in Fig. 2, the iteration

stops at  $t = k\Delta t$ . The mean time to place the maintenance request MTTM in Eq. (2) is now calculated as follows:

$$h(t) = \int_0^M f_Y^b(y, t) dy \quad t = 0, \Delta t, 2\Delta t, \dots, k\Delta t \quad (9)$$

$$MTTM = \int_0^{\infty} h(t) dt \quad (10)$$

where  $h(t)$  denotes the probability that the system has not reached maintenance threshold  $M$  at time  $t$  (white-colored area in Fig. 2). It is assumed that the maintenance alarm is triggered when the degradation level reaches  $M$  for the first time (i.e.,  $y(t) \geq M$ ) and does not return to below maintenance threshold  $M$  afterwards. Thus, it is important to note that the probability that the system surpasses maintenance threshold  $M$

at time  $t$  (i.e.,  $\int_M^{\infty} f_Y^b(y, t) dy$ ), highlighted in the gray color in Fig. 2,

should be removed before updating the PDF at time  $t + \Delta t$  (i.e.,  $\int_M^{\infty} f_Y^b(y, t + \Delta t) dy$ ).

Since  $f_Y^b(y, t + \Delta t)$  is only updated based on  $\int_0^M f_Y^b(y, t) dy$  (i.e.,

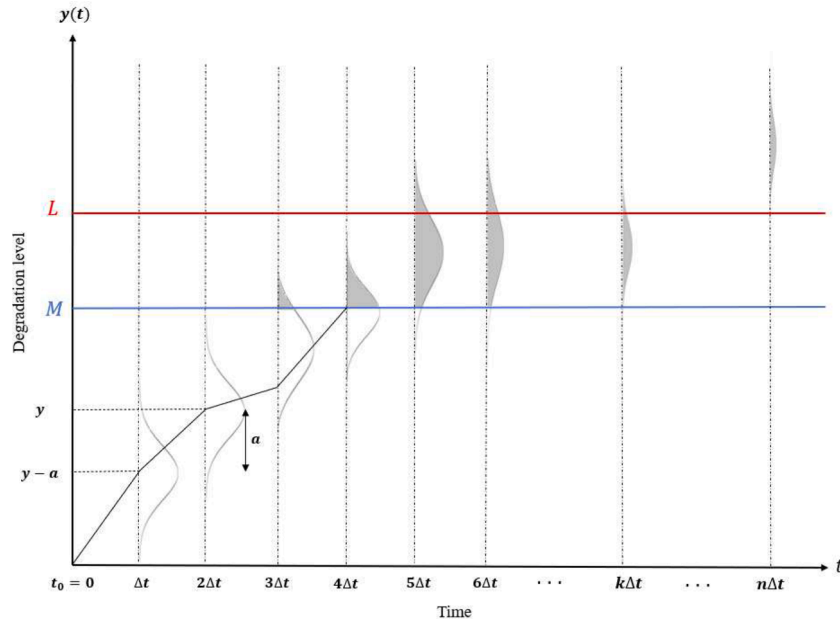


Fig. 2. Numerical propagation of PDF at different time steps when  $y(t) \in [0, M]$ .

e., the white area of the PDFs in Fig. 2),  $\int_M^\infty f_Y^b(y, t) dy$  (i.e., the gray area of the PDFs) becomes smaller and eventually tends to zero.

**Case 1-II) degradation level above maintenance threshold M.** When the degradation level passes maintenance threshold M for the first time, the maintenance alarm is triggered and the mobilization for maintenance is started. This time is labeled  $t_M = \inf\{t : y(t) \geq M\}$ . It is assumed that there is a lead time  $T_L$  from when the maintenance alarm is triggered  $t_M$  until the renewal is completed  $t_C$ . The initial degradation level in this case is  $y(t_M) = M$  which means  $\Pr(y(t) = t_M) = M = 1$ . Eq. (11) is used to update the PDF at each time step when the degradation level is above M.

$$f_Y^a(y, t + \Delta t) = \int_{-\infty}^\infty f_Y^a(y - a, t)g(a) da \quad (11)$$

Fig. 3 is an illustration of the numerical process in Case 1-II when  $y(t) \in [M, L]$  along with a realization of a degradation process. It presents how the PDF of degradation level  $y$  is updated over time throughout the degradation process. Since Case 1-II is specifically related to  $y(t) \in [M, L]$ , we did not illustrate the degradation level  $y$  beyond the point where it reaches the failure threshold L. However, the propagation of PDF of  $y$  continues until  $t = t_M + T_L$ .

The initial PDF of  $y$  at time  $t = t_M + \Delta t$  (i.e.,  $f_Y^a(y, t_M + \Delta t)$ ) is a Normal distribution on the increments with the mean and standard deviation  $M + (\mu \cdot \Delta t)$  and  $\sigma\sqrt{\Delta t}$  respectively. The PDF is then updated for the period of lead time ( $T_L$ ) to calculate the probability of failure  $\Pr(t_F < t_C | M)$  and expected downtime  $E[DT | M]$ .

It is assumed that the failure occurs when the degradation level  $y$  hits the failure threshold L for the first time. Eq. (13) and Eq. (14) show how to calculate the probability of failure and expected downtime, where  $m(t)$  in Eq. (12) is the system's failure probability at time  $t$  (i.e., the gray-colored area in Fig. 3). It is assumed that once the degradation level  $y$  exceeds L, it does not return to below that threshold. Therefore, the probability that the system crosses L for the first time at time  $t$  (i.e.,  $\int_L^\infty f_Y^a(y, t)$ ), highlighted in gray color in Fig. 3, should be first stored in

a vector (i.e.,  $m(t)$  in Eq. (12)), and then removed before updating the PDF at time  $t + \Delta t$  (i.e.,  $f_Y^a(y, t + \Delta t)$ ).

$m(t) = \int_L^\infty f_Y^a(y, t) dy$   $t = t_M + \Delta t, t_M + 2\Delta t, \dots, t_M + T_L$  (12)

$$\Pr(t_F < t_C | M) = \int_{t=t_M+\Delta t}^{t=t_M+T_L} m(t) dt \quad (13)$$

$$E[DT | M] = \int_{t=t_M+\Delta t}^{t=t_M+T_L} [T_L - t] m(t) dt \quad (14)$$

The expected cost in Eq. (2) can now be computed using Eqs. (10), (13), and (14).

### 2.1.2. Comparison with analytical solution

In Case 1, the impact of external shocks is excluded from the model. Let us assume that the degradation process is continuously monitored without any uncertainty, and it follows a linear Wiener process. A failure occurs if the degradation level  $y(t) \geq L$  for the first time. As previously mentioned, in a Wiener process, the distribution of the first hitting time to a fixed threshold follows an IG distribution. Considering one maintenance cycle, if the degradation level  $y(t)$  hits the maintenance threshold M at time  $t$  (i.e.,  $y(t) = M$ ), the maintenance alarm is triggered and the mobilization for maintenance is started.  $RUL_m$  is defined as the time from  $t = t_M$  until a failure occurs (i.e.,  $t_F$ ).  $RUL_m$  is then IG distributed with the parameters  $\nu_M = \frac{L-M}{\eta}$  and  $\kappa_M = \frac{(L-M)^2}{\sigma_B^2}$  where  $\eta$  and  $\sigma_B$  are the drift and diffusion parameters of the Wiener process. The MTTM is then equal to  $\frac{M}{\eta}$ , while  $\Pr(t_F < t_C | M)$  and  $E[DT | M]$  are obtained according to Eqs. (15) and (16).

$$\Pr(t_F < t_C | M) = \int_{t=t_M+\Delta t}^{t=t_M+T_L} f_T(t; \nu_M, \kappa_M) dt = F_T(t; \nu_M, \kappa_M) \quad (15)$$

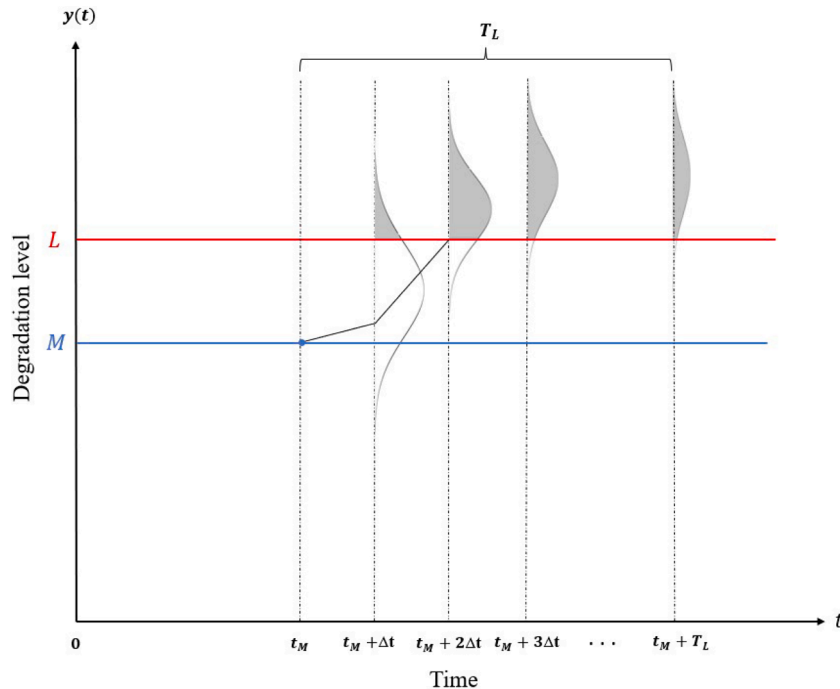


Fig. 3. Numerical propagation of PDF at different time steps when  $y(t) \in [M, L]$ .

$$E[DT|M] = \int_{t=M+\Delta t}^{t=M+T_L} [T_L - t] f_T(t; \nu_M, \kappa_M) dt \quad (16)$$

where  $f_T(t; \nu_M, \kappa_M)$  and  $F_T(t; \nu_M, \kappa_M)$  are the PDF and cumulative distribution function (CDF) of IG distribution given that  $y(t) = M$ . Eq. (17) presents the PDF of IG distribution.

$$f_T(t; \nu, \kappa) = \sqrt{\frac{\kappa}{2\pi t^3}} \exp\left\{-\frac{\kappa(t-\nu)^2}{2\nu^2 t}\right\} \quad (17)$$

## 2.2. Case 2: modeling – Gradual degradation and external shocks

### 2.2.1. Numerical approach

Case 2 considers the probability of external shocks occurring at each time step  $\Delta t$  in addition to the system aging. Taking shocks into account with different stochastic magnitudes or impacts on the degradation level makes the model more realistic. In this case, IG distribution is no longer applicable to model the system deterioration process and, thus, the numerical solution of the model is proposed and compared with MCS.

The model consists of two parts (i.e., Case 2-I and Case 2-II). Case 2-I is when the degradation level  $y$  is below maintenance threshold  $M$  (i.e.,  $y(t) \in [0, M]$ ). In this case, a shock may occur below the maintenance threshold  $M$  with a stochastic magnitude. The three different situations that can happen as a result are listed below and illustrated in Fig. 4:

- (a) The magnitude of the shock is small, and the degradation level remains below the maintenance threshold (i.e.,  $y \leq M$ ).

- (b) The magnitude of the shock is medium, and the degradation level exceeds the maintenance threshold; however, it remains below the failure threshold (i.e.,  $M < y < L$ ).
- (c) The magnitude of the shock is large, and the degradation level exceeds the failure threshold (i.e.,  $y \geq L$ ).

Case 2-II is when the degradation level  $y$  is above maintenance threshold  $M$  (i.e.,  $y(t) \in [M, L]$ ). A shock may occur during the lead time  $T_L$ . This means that the degradation level  $y$  in this case is above the maintenance threshold  $M$  since the mobilization for maintenance has already started, but renewal is not completed yet. The two situations that can occur as a result are listed below and illustrated in Fig. 5:

- (a) The magnitude of the shock is small, and the degradation level remains between the maintenance threshold and the failure threshold (i.e.,  $M < y < L$ ).
- (b) The magnitude of the shock is large, and the degradation level exceeds the failure threshold (i.e.,  $y \geq L$ ).

The numerical approach to formulate the expected cost is presented in the next section. Similar to Case 1, the purpose is to calculate the PDF of the degradation level  $y$  at time  $t + \Delta t$  (i.e.,  $q_Y(y, t + \Delta t)$ ) as a function of the PDF of  $y$  at time  $t$  (i.e.,  $q_Y(y, t)$ ). Once we calculate  $q_Y(y, t)$  at time  $t$ , we can use the law of total probability to combine  $f_Y(y, t)$  and  $q_Y(y, t)$  to obtain the final PDF of  $y$  (i.e.,  $w_Y(y, t)$ ) in Case 2, accounting for both internal degradation modelled by the Wiener process and stochastic shocks modelled by HPP.

Case 2-I) degradation level below maintenance threshold  $M$ . In this sec-

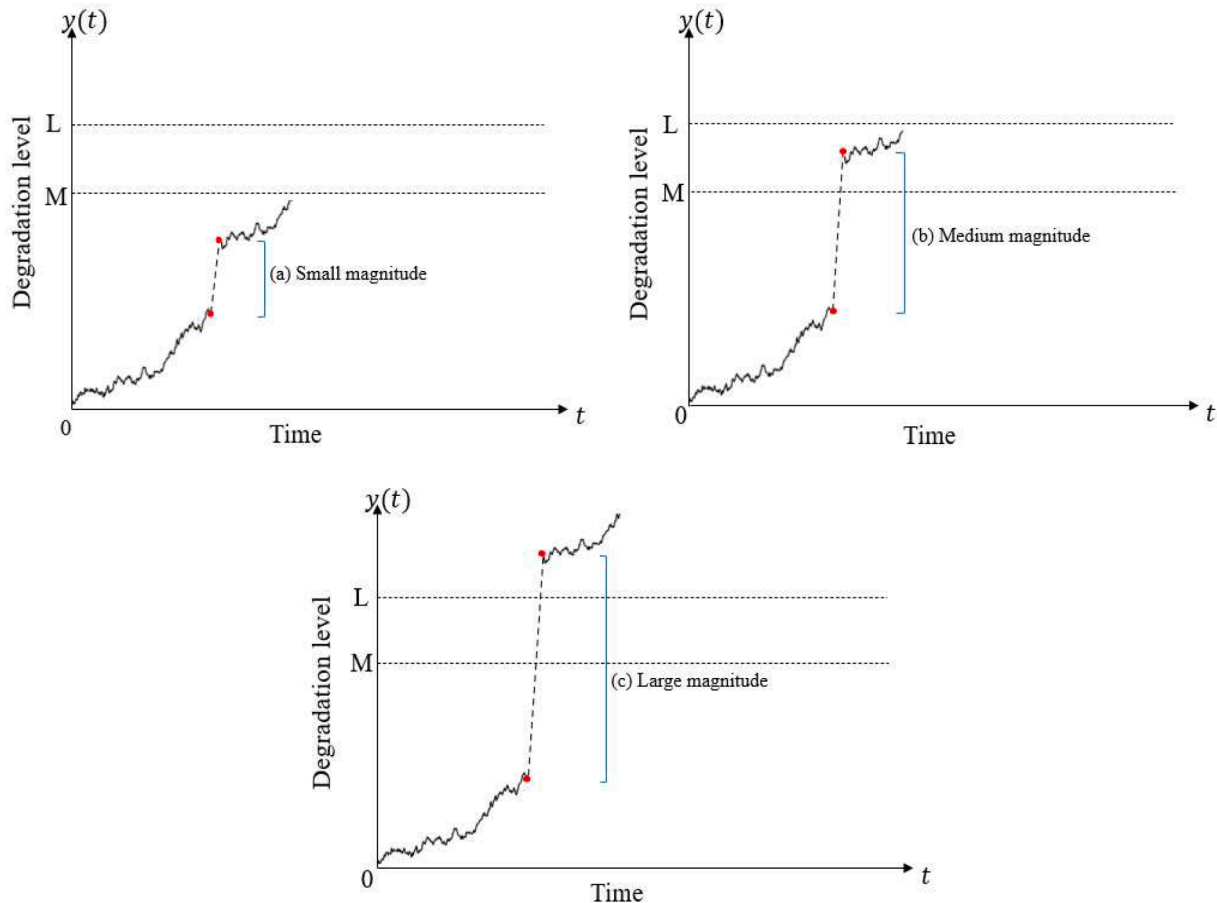


Fig. 4. A schematic of the three alternatives when an external shock occurs below maintenance threshold  $M$  and the degradation level is affected by a shock with small, medium, and large magnitude. The dashed lines represent the impact of the shock on the degradation level.



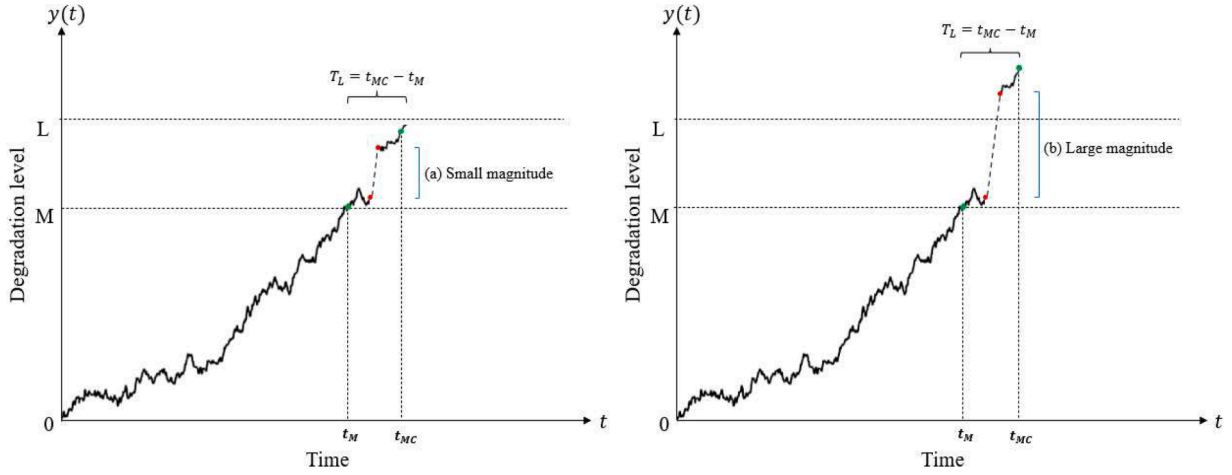


Fig. 5. A schematic of the two alternatives when an external shock occurs above maintenance threshold  $M$  and the degradation level is affected by a shock with small and large magnitude. The dashed lines represent the impact of the shock on the degradation level.

tion, it is assumed that the system's degradation process  $y(t)$  is still a non-monotonic Wiener process, while external shocks with stochastic magnitudes can occur randomly throughout the degradation process. A shock has a random magnitude  $s$  and can increase the degradation level by a random extent. We further assume that the shock magnitude  $s$  is independent of  $y(t)$  and follows a Gamma distribution with shape and scale parameters  $\alpha$  and  $\lambda$  respectively. If a shock occurs, the PDF of the degradation level  $y$  at time  $t + \Delta t$  can be given as follows:

$$q_Y^b(y, t + \Delta t) = \int_0^\infty q_Y^b(y - s, t) u(s) ds \quad (18)$$

where  $u(s)$  is the PDF of stochastic shocks' magnitudes (i.e.,  $u(s) \sim \text{Gamma}(s; \alpha, \lambda)$ ) and  $q_Y^b(y - s|t)$  is the PDF of the degradation level before the shock occurs at time  $t$ . The final PDF of  $y$  at time  $t$  in Case 2-I when  $y$  is below the maintenance threshold  $M$  (i.e.,  $y(t) \in [0, M]$ ), considering both gradual degradation and external shocks, is then as follows:

$$w_Y^b(y, t) = (1 - \rho\Delta t) f_Y^b(y, t) + \rho\Delta t q_Y^b(y, t) \quad (19)$$

where  $f_Y^b(y, t_i)$  and  $q_Y^b(y, t_i)$  are calculated using Eq. (8) and Eq. (18) respectively. Since a shock might bring the system either to a fault state (i.e.,  $y \geq L$ ) or a state between the maintenance threshold and failure threshold (i.e.,  $M < y < L$ ), the probability that the system passes maintenance threshold  $M$  at time  $t$  (i.e., gray-colored in Fig. 2) is cumulatively stored in a vector  $\varphi_Y(y) = \int_0^\infty w_Y^b(y, t) dt$  for  $y \geq M$  over time  $t$ , and then removed before updating the PDF at time  $t + \Delta t$ . Eq. (21) shows how to calculate MTTM as a function of the maintenance threshold  $M$ .

$$h(t) = \int_0^M w_Y^b(y, t) dy \quad (20)$$

$$\text{MTTM} = \int_0^\infty h(t) dt \quad (21)$$

**Case 2-II degradation level above maintenance threshold  $M$ .** When the degradation level crosses the maintenance threshold  $M$  and the mobilization for maintenance is started, the initial PDF of  $y$  at time  $t = t_M + \Delta t$  (i.e.,  $q_Y^a(y, t_M + \Delta t)$ ) will be as follows:

$$q_Y^a(y, t = t_M + \Delta t) = \varphi_Y(y) \quad (22)$$

It is important to note that  $\int_M^\infty \varphi_Y(y, t) dy = 1$  when  $t \rightarrow \infty$ , since the numerical iteration process to update the PDF of  $y$  in Case 2-I stops at some time  $t$  where the probability of not reaching the maintenance threshold  $M$  is equal to zero (i.e.,  $\int_0^M q_Y^b(y, t) dy = 0$ ). Eq. (23) is used to update the PDF of  $y$  at each time step for the period of lead time  $T_L$  which initially starts with the PDF in Eq. (22).

$$q_Y^a(y, t + \Delta t) = \int_0^\infty q_Y^a(y, t) u(s) ds \quad (23)$$

To obtain the final update of the PDF of  $y$  when  $y$  is above the maintenance threshold  $M$ , we use law of total probability which combines Cases 1 and 2 to account for the gradual degradation and external stochastic shocks in each time interval  $\Delta t$ . Eq. (24) represents the final PDF of the degradation level  $y$  at time  $t$  when  $y(t) \in [0, M]$  (i.e.,  $w_Y^a(y, t)$ ):

$$w_Y^a(y, t) = (1 - \rho\Delta t) f_Y^a(y, t) + \rho\Delta t q_Y^a(y, t) \quad (24)$$

where  $f_Y^a(y, t)$  is calculated using Eq. (11) and  $q_Y^a(y, t)$  is obtained from Eq. (23). Similar to the numerical approach in Case 1, the probability that the system crosses  $L$  for the first time at time  $t$  (i.e.,  $\int_L^\infty w_Y^a(y, t)$ , highlighted in gray color in Fig. 3, should be first stored in a vector (i.e.,  $m(t)$  in Eq. (25)), and then removed before updating the PDF at time  $t + \Delta t$  (i.e.,  $w_Y^a(y, t + \Delta t)$ ).

Eqs. (26) and (27) are used to calculate the probability of failure and expected downtime during lead time.

$$m(t) = \int_L^\infty w_Y^a(y, t) dy \quad t = t_M + \Delta t, t_M + 2\Delta t, \dots, t_M + T_L \quad (25)$$

$$\Pr(t_{f|t_{MC}}|M) = \int_{t=t_M+\Delta t}^{t=t_M+T_L} m(t) dt \quad (26)$$

$$E[DT|M] = \int_{t=t_M+\Delta t}^{t=t_M+T_L} [T_L - t] m(t) dt \quad (27)$$

The cost function in Eq. (2) can now be computed using the parameters in Eqs. (21), (26), and (27).

### 2.2.2. Comparison with Monte-Carlo simulation

The Monte-Carlo simulation is used to verify the numerical approach in Case 2. In MCS, the degradation process is sampled for  $10^4$  number of times and MTTM,  $\Pr(t_F(t_C|M))$ , and  $E[DT|M]$  are calculated for maintenance threshold  $M \in [0, L]$ . Algorithm and Algorithm are the pseudo-codes.

## 3. Results

### 3.1. Numerical example

Without loss of generality, a numerical example with the following assumptions is used to illustrate the proposed model:

- The degradation process is modelled by a non-monotonic Wiener process with parameters  $\eta = 0.3$  and  $\sigma_B = 0.1$ .
- The failure threshold is  $L = 30$ .
- The lead time is  $T_L = 4$ .
- The shocks follow a homogenous Poisson process with the intensity rate  $\rho = 0.1$ .
- The magnitudes of random shocks follow a Gamma distribution with shape and scale parameters  $\alpha = 9$  and  $\lambda = 0.5$  respectively.
- The cost of replacement, cost of failure, and cost of downtime per unit time are 500, 300, and 200 respectively.

#### 3.1.1. Case 1

According to Case 1, where the degradation is described by a non-monotonic Wiener process and the shock is excluded from the model, MTTM,  $\Pr(t_F(t_C|M))$ ,  $E[DT|M]$ , and the expected cost function in Eq. (2) are calculated numerically and analytically to find the optimal maintenance threshold  $M^*$  with the minimum expected cost rate  $C(M^*)$ . Fig. 6 shows the expected cost versus different maintenance thresholds for the numerical example.  $M^*$  and  $C(M^*)$  are 28.3 and 5.15 respectively.

#### 3.1.2. Case 2

In Case 2, the expected total cost versus maintenance threshold  $M$  for our numerical example is computed, compared with MCS, and presented in Fig. 7. In our case, although there is a small deviation in numerical solution and MCS due to numerical approximations error, the optimal maintenance threshold  $M^*$  is the same in both approaches (i.e.,  $M^* = 23$ ).

Generally, MCS method is widely used in practice and conceptually easy to apply, while the numerical scheme provides more accurate re-

sults with short computation time [26]. In MCS, generating numerous samples leads to a more accurate estimation of results and better simulation performance, while it increases the computation time. Some factors, including the desired accuracy, efficiency of the code, problem size, and complexity, can also affect the computation time in both MCS and numerical solutions. In terms of computation time, our numerical scheme takes 270 s, whereas MCS with  $10^4$  number of samples takes approximately 200 s. While MCS with  $10^4$  replications may be faster than the numerical scheme, it provides less accuracy. To achieve better accuracy, a large number of replications are required. Running MCS with  $10^6$  replications increases the accuracy, but takes almost four times longer than the numerical scheme (i.e., 960 s). Thus, the numerical framework is still preferable in situations where accuracy is crucial, since it provides more accurate results in less time compared to MCS.

According to Fig. 8, incorporating external shocks in the model leads to significant changes in probability of failure. The pure Wiener process can not capture the impact of external shocks and underestimates the system's failure probability. Thus, it makes it challenging to accurately assess risk and make effective maintenance decisions. However, since the shock model accounts for unexpected events, it gives a more reliable estimation of failure probability, and thus is more appropriate to model the real-world degradation behavior of systems.

### 3.2. Numerical stability

Numerical stability is a common challenge in employment of numerical methods that involve a discretization process. Discretization is a source of instability and is mostly required to solve the differential equations of systems on a computer [1]. Understanding the stability behavior in numerical algorithms can provide guidance in adjusting numerical parameters and, thus, a more accurate and reliable prediction result. One of the approaches to deal with instability in numerical approximations is time step selection [18]. If the time step is either too large or too small, instability can occur due to, for instance, discretization error. In this work, different time steps (i.e.,  $\Delta t = 0.1, 0.2, 0.3, \dots, 0.9, 1$ ) have been used to solve the numerical problem. When the time step is too large (e.g.,  $\Delta t = 1$ ), the numerical solution can become unstable. Thus, reducing the time step can be helpful to reduce the discretization error. However, if the time step decreases too much, other sources of errors may become dominant, such as round-off error due to a large number of numerical operations required to compute the solution. This can lead to a situation where decreasing the time step further may not necessarily improve the solution's accuracy, but instead increase the

### Algorithm 1

Monte-Carlo simulation, MTTM.

---

**Input:** Normal distribution parameters  $(\mu, \sigma)$ , Gamma distribution parameters  $(\alpha, \lambda)$ , homogeneous Poisson process intensity factor  $(\rho)$ , Number of simulations  $(nSim)$ , Failure threshold  $(L)$ , and time step  $(\Delta t)$

**for**  $m = 1$  **to**  $M_{max}$  **do**

**for**  $n = 1$  **to**  $nSim$  **do**

$y_0 = 0$

$t_0 = 0$

**while**  $y \leq M$  **do**

      ◦ Generate a random number between 0 and 1,  $R$ .

      ◦ Generate two random numbers from Gamma distribution with  $\alpha, \lambda$  parameters,  $U \sim Gamma(\alpha, \lambda)$ , and Normal distribution with  $\mu, \sigma$  parameters,  $W \sim Normal(\mu, \sigma)$

**if**  $R \leq \rho \times \Delta t$  **do**

$y = y + W + U$

**else**

$y = y + W$

**end if**

$T = T + \Delta t$

**end while**

$T_{vector}(n, 1) = T$

**end for**

$MTTM_{simulation}(m) = mean(T_{vector})$

**end for**

**Output:** The output is the MTTM or the mean time it takes for the simulated degradation paths to cross the maintenance threshold  $M$ .

---

**Algorithm 2**

Monte-Carlo simulation,  $\Pr(t_{f}(t_{MC}|M)$  and  $E[DT|M]$ .

```

Input: The inputs for this algorithm are the same as inputs for Algorithm 1, in addition to lead time ( $T_L$ )
for  $n = 1$  to  $nSim$  do
  for  $t = 1$  to  $T_L$  do
     $y_0 = 0$ 
     $t_0 = 0$ 
    ◦ Generate a random number between 0 and 1,  $R$ .
    ◦ Generate two random numbers from Gamma distribution with  $\alpha, \lambda$  parameters,  $U \sim Gamma(\alpha, \lambda)$ , and Normal distribution with  $\mu, \sigma$  parameters,  $W \sim Normal(\mu, \sigma)$ 
    if  $R \leq \rho \times \Delta t$  do
       $y(t) = y(t) + W + U$ 
    else
       $y(t) = y(t) + W$ 
    end if
    ◦ Count the number of simulated paths that have a degradation level larger than  $L$  (i.e.,  $y(t) \geq L$ ) at a specific time  $t$  and divide it by  $nSim$ , (i.e.,  $P(f) = \frac{\text{Count the number of times that } y(t) \geq L \text{ for the first time}}{nSim}$ )
  if  $y(t) \geq L$  do
    ◦ Find the time that  $y(t) \geq L$ , i.e.,  $t_{failure}$ 
    ◦ Calculate downtime as  $DT = T_L - t_{failure}$ 
  else
    ◦  $DT = 0$ 
  end if
  ◦ Expected downtime =  $\sum_1^{nSim} DT$ 
end for
end for
Output: The output is the probability of failure during lead time  $\Pr(t_{f}(t_C|M)$  and the expected downtime  $E[DT|M]$  given a maintenance threshold  $M$ .
  
```

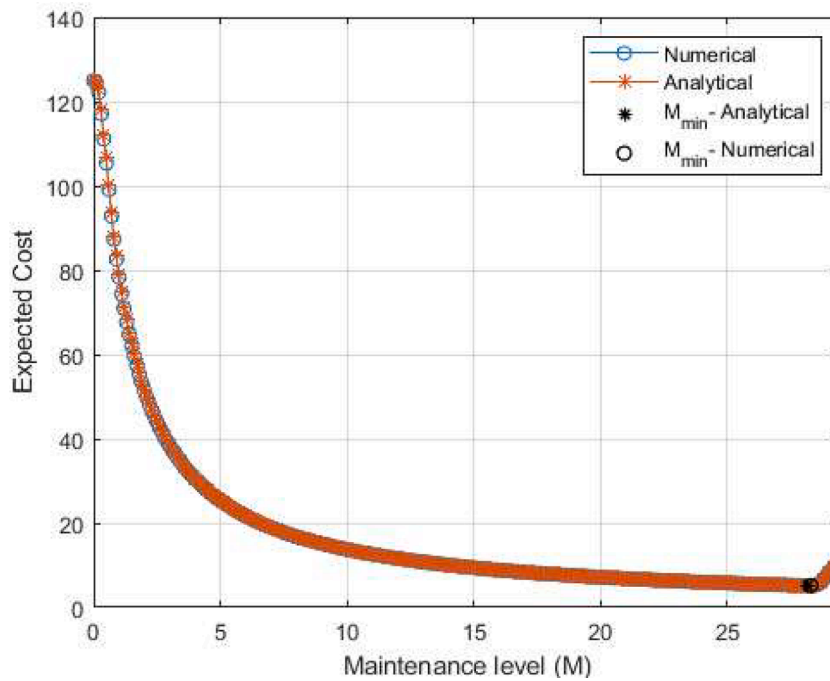


Fig. 6. Expected cost vs maintenance threshold in Case 1.

overall error and computational cost. Finding an acceptable time step requires a balance between computational cost and the desired accuracy.

In this case, reducing the time step from  $\Delta t = 1$  to  $\Delta t = 0.4$  decreases the overall error significantly. However, further reducing the time step from  $\Delta t = 0.4$  to  $\Delta t = 0.3$  increases the overall error due to round-off error accumulation, which can offset the benefit of smaller time steps. Decreasing the time step further again from  $\Delta t = 0.3$  to  $\Delta t = 0.1$  leads to a lower round-off and, consequently, overall error. Fig. 9 presents the expected cost versus maintenance threshold  $M$  with different time steps. The time step  $\Delta t = 0.1$  provides the lowest deviation or overall error with MCS. However,  $\Delta t = 0.2$  is also acceptable, leading to the same result while taking less computation time compared to  $\Delta t = 0.1$ .

3.3. Experimental data

A real-time experimental dataset is collected in Reliability, Availability, Maintenance, and Safety (RAMS) laboratory at Norwegian University of Science and Technology (NTNU) to illustrate the applicability of the proposed model. There are 10 run-to-failure datasets from 10 ball bearings, which are a type of rolling-element bearings that use balls to maintain the separation between the bearing inner and outer races. The bearings are degraded by contamination, which is the result of pouring a mixture of Silicon carbide solid particles and lubricant onto the bearing at regular time intervals until the amplitude of the acceleration, in a horizontal direction, crosses the level of 10 g. The details of the setup and the experiments can be read in Tajiani and Vatn [33].

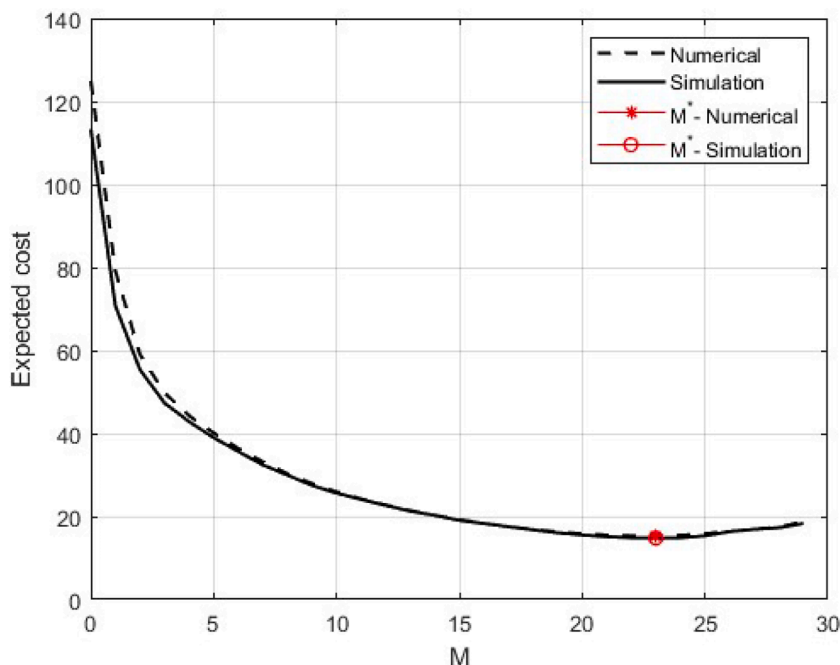


Fig. 7. Expected cost vs maintenance threshold for Case 2.

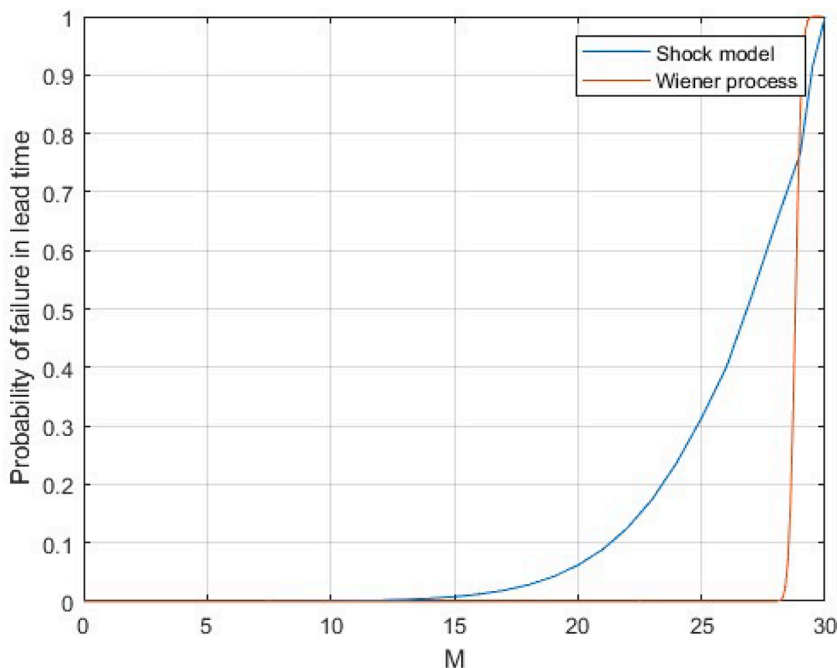


Fig. 8. Probability of failure in lead time for Wiener process (Case 1) and shock model (Case 2).

In each experiment, the samples of horizontal acceleration signals are collected every five minutes, and the lifetime of bearing is a batch of the collected samples. The horizontal acceleration samples are then decomposed into time-based segments called intrinsic mode functions (IMFs) and the statistical features such as kurtosis, crest factor, and root mean square (RMS) are extracted from the different IMFs as condition indicators. There have been various studies on different features and their associated capability for condition monitoring and remaining useful life (RUL) prediction of bearings. Based on our previous research in Tajiani and Vatn [33], the RMS feature extracted from the first IMF with the highest frequency is the most suitable health indicator (HI) for

degradation modeling and RUL prediction with the lowest prediction error. Thus, it has been selected as the HI for the optimization of the maintenance threshold  $M$ . Fig. 10 shows the RMS features from the first IMF of 10 experimental bearings, which show increasing trends over the bearing lifetime.

In real-life applications, it is often possible to detect external shocks, caused by natural disasters, harsh environment conditions, and seasonal variations. It is primarily more straightforward by collecting and analyzing historical data, having knowledge of the system, and comparing the system degradation patterns at different time periods. In industries, this type of data is often available, and one can differentiate

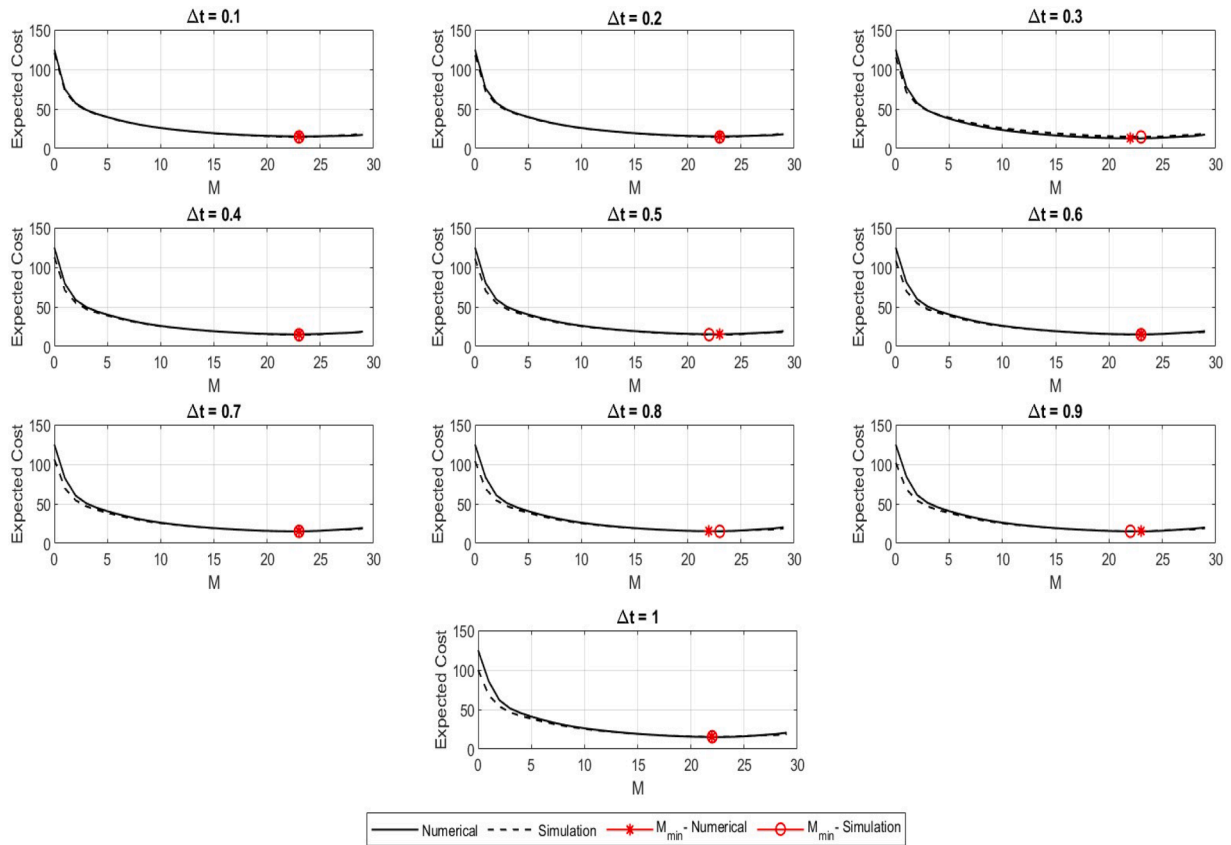


Fig. 9. Expected cost vs maintenance threshold with different time steps.

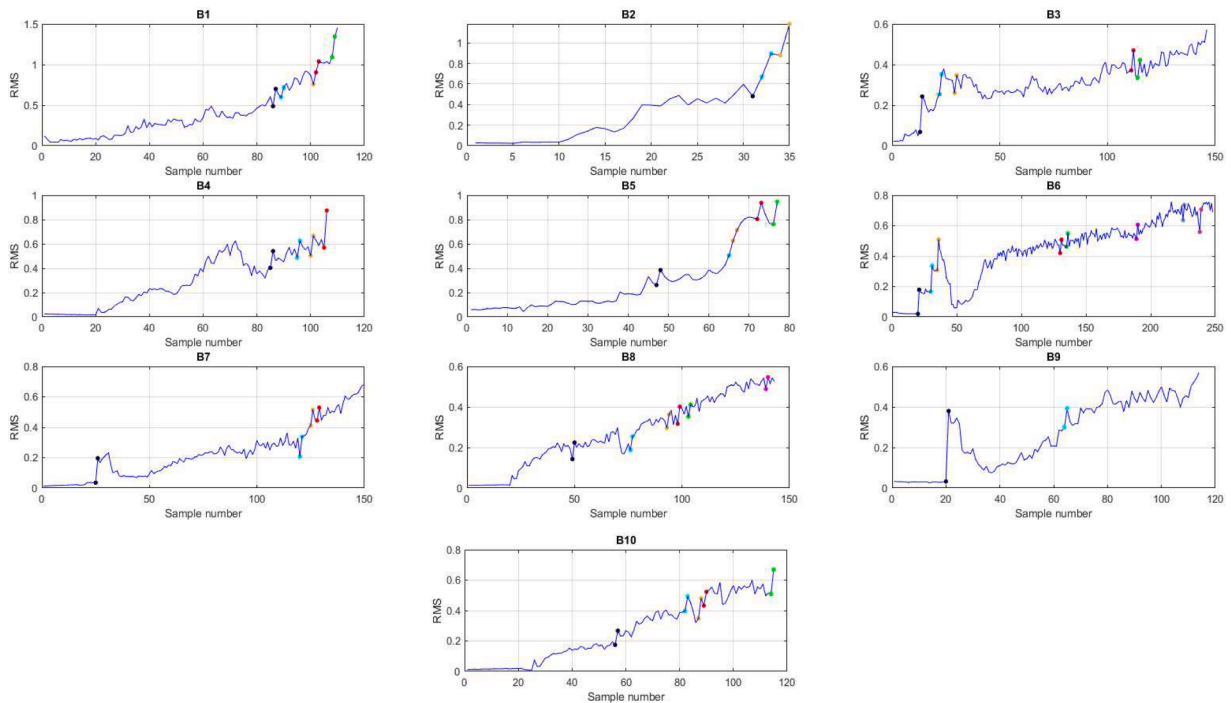


Fig. 10. RMS degradation paths for experimental bearings. Each two consecutive colored datapoints represent the shock increment.

between the shocks and the system’s gradual degradation by tracking work orders and analyzing maintenance records.

In our case, since particles contamination has been used to accelerate the bearings degradation, it is somewhat challenging to detect whether

the Silicon carbide particles contributed to shocks or not. In addition, in a more controlled environment like a laboratory, the experiments are carried out under the same operating conditions, and the influence of some external random shocks such as extreme weather conditions is

minimized. In our experimental dataset, it is assumed that the shocks have only positive magnitudes which increase the degradation level to a random extent, and the negative increments correspond to the system's gradual degradation modelled by the Wiener process. This assumption is valid for some external factors such as operational loads. The operational load on roller bearings is a factor that increases the degradation level (i.e., vibration) with only positive magnitudes, and negatively affects its lifespan and performance. The following algorithm is used to differentiate the increments corresponding to gradual degradation and shocks in bearing dataset.

A linear Wiener process and a HPP are used to capture the behavior of gradual degradation and external shocks in the deterioration paths presented in Fig. 10, respectively. The magnitudes of the shocks (i.e., shock impacts on degradation level) are modelled by a Gamma distribution. The parameters of both Wiener process and Gamma distribution are estimated using Maximum Likelihood Estimation (MLE) and summarized in Table 1. Additionally, Table 1 shows the intensity rate of HPP, which is the number of shocks divided by the number of samples of a bearing. The lead time is assumed to be constant for the bearings, and it is equal to 25 samples. Given that the time interval between each two consecutive samples is five minutes, the lead time can be interpreted in time unit as well.

The expected cost is now calculated given a maintenance threshold  $M$ , and the optimal maintenance threshold  $M^*$ , which minimizes the expected cost, is obtained numerically for the different bearings. Fig. 11 shows the expected cost versus maintenance threshold using two different shock detection thresholds (i.e.,  $1.5\sigma$  and  $2\sigma$ ) for distinguishing the external shocks. Determining an appropriate threshold to detect shocks depends on the context, data characteristics, and desired risk tolerance. In some systems, if missing a shock has severe consequences, defining a more conservative threshold is required to capture a broader range of potentially significant events. Table 2 summarizes  $M^*$  and  $C(M^*)$  for the bearings.

The different model parameters and the lifetime of the bearings lead to different maintenance strategies (i.e., run-to-failure, request maintenance early at the life stage, etc.). For instance, in B2, the lead time is large compared to the bearing lifetime, which gives a higher probability of failure during lead time. Therefore, the optimal maintenance threshold to place the maintenance request is at the beginning of the experiment. However, in B10, the maintenance strategy according to  $1.5\sigma$  is "run-to-failure", which means that the bearing can be operated until it fails or breaks down, while, according to  $2\sigma$  threshold, the optimal maintenance threshold is 0.45 where more than half of the bearing lifespan has elapsed. Setting a lower threshold for detection of shocks provides a more sensitive analysis of any deviations from the system expected behavior.

### 3.4. Impact of shock detection threshold on expected cost

The thresholds  $1.5\sigma$  and  $2\sigma$  to identify shocks on experimental data are chosen heuristically based on the data characteristics. However, to evaluate the performance of shock detection threshold, 75 degradation processes including both gradual degradation increments and shocks are simulated using the parameters in Section 3.1 and Algorithm 3. The index of shocks (i.e., the location of shocks in the degradation process) are recorded in a vector throughout the simulation process. Different

shock detection thresholds from  $0.1\sigma$  to  $3\sigma$ , where  $\sigma$  is the standard deviation of the degradation increments in a deterioration process, have been tested on the simulated data, to identify how precise they are in capturing the shocks. Eq. (28) presents the shock detection rate (SDR) to evaluate the performance of the thresholds.

$$SDR = \frac{\text{Number of shocks detected}}{\text{Total number of shocks}} \tag{28}$$

Fig. 12 shows the average of SDR over all simulated degradation processes versus shock detection threshold. The thresholds  $1.5\sigma$  and  $2\sigma$  can, on average, detect 98.5% and 92.1% of the shocks, respectively. According to Fig. 12, fewer shocks are detected when the threshold increases. This is a trade-off between sensitivity and precision [17]. A lower threshold means the model is more sensitive to shocks; however, it might include false positives or increments that are incorrectly identified as shocks. On the other hand, a higher threshold means the shock detection criteria is stricter and the shocks have more significant deviation from the mean of the increments. A higher threshold increases precision and reduces the false positives, while there is a probability of missing some real shocks with smaller magnitudes. Selecting the right balance between sensitivity and precision depends on the application context and can be adjusted based on the criticality of missing shocks.

Additionally, to evaluate the impact of the shock detection threshold on the expected cost, we used the same simulated degradation processes with known shock indexes. The parameters  $\eta$ ,  $\sigma_B$ ,  $\alpha$ ,  $\lambda$ ,  $\rho$  have been estimated using MLE and the expected cost  $C_\infty(M)$  for maintenance threshold  $M$  is obtained numerically for each simulated degradation process. Since the actual arrangement of the degradation process with respect to shocks and gradual degradation increments is known,  $M^*_{Actual}$  is used to denote the optimal maintenance threshold with minimum expected cost in this case. Similarly, the thresholds  $1\sigma$ ,  $2\sigma$ , and  $3\sigma$  are employed to distinguish shocks and calculate the expected cost  $C_\infty(M)$  for maintenance threshold  $M$ . Fig. 13 shows the average result over all simulated degradation processes. The optimal maintenance thresholds (i.e.,  $M^*$ ) are marked in a black color.

According to Fig. 13, the optimal maintenance threshold and its associated expected cost for the thresholds  $1\sigma$  and  $2\sigma$  are close to the actual result. This means that these two thresholds have a balanced sensitivity that results in a more reliable estimation of  $M^*$  and its associated expected cost. However, using the  $3\sigma$  threshold to detect shocks leads to an underestimation of the expected cost and it suggests a larger maintenance threshold. This means that it delays the initiation of maintenance and negatively impacts the decision-making process. One of the reasons for this is that the  $3\sigma$  threshold identifies the most extreme events as shocks and, thus, neglects the smaller shocks. Although the smaller shocks might not have a significant impact individually, their cumulative effect can be critical over time and contribute to the overall system degradation. The findings in this section are based on a limited number of simulated datasets and the time step  $\Delta t = 1$  is used due to high computation costs. Despite these limitations, the overall trend of expected cost versus maintenance threshold demonstrated stability after approximately 50 simulated degradation processes.

## 4. Discussion

Some of the maintenance optimization models are often suitable for

**Table 1**  
Parameters of Wiener process, Gamma distribution, and the intensity rate of HPP.

	B1	B2	B3	B4	B5	B6	B7	B8	B9	B10
$\eta$	0.0144	0.0199	0.0042	0.0065	0.0113	0.0029	0.0048	0.0040	0.0052	0.0049
$\sigma_B$	0.0645	0.0475	0.0324	0.0366	0.0494	0.0359	0.0276	0.0236	0.0410	0.0382
$\alpha$	12.5489	25.0876	13.1046	8.6036	17.9423	10.3389	17.8410	46.7518	2.6118	18.7613
$\lambda$	0.0138	0.0096	0.0083	0.0216	0.0073	0.0126	0.0067	0.0015	0.0842	0.0061
$\rho$	0.0455	0.0857	0.0342	0.0377	0.0649	0.0323	0.0267	0.0420	0.0175	0.0435

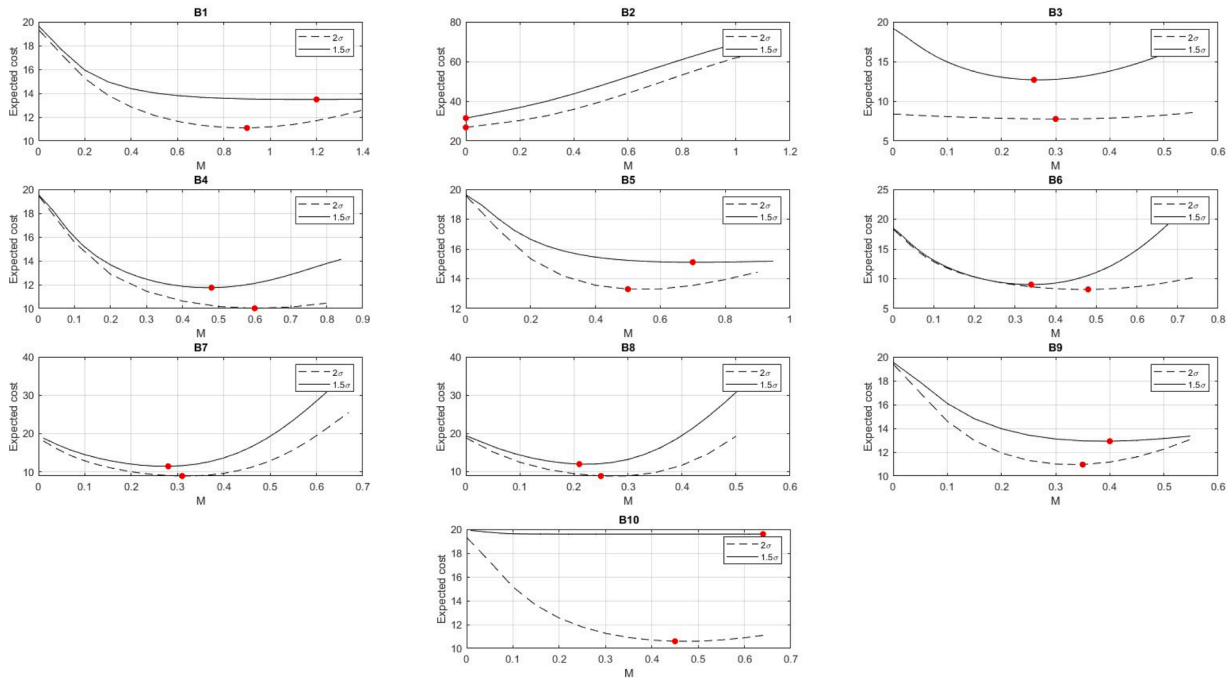


Fig. 11. Expected cost rate over maintenance limit for different bearings.

Table 2

Optimal maintenance threshold  $M^*$  with minimum expected costs  $C(M^*)$  for the bearings considering a  $2\sigma$  threshold.

Bearing	$M^*$	$C(M^*)$
B1	0.9	11.09
B2	0	26.8
B3	0.3	7.76
B4	0.6	10.01
B5	0.5	13.3
B6	0.48	8.2
B7	0.31	8.87
B8	0.25	8.77
B9	0.35	10.96
B10	0.45	10.59

systems that are only subject to gradual degradation or aging [28,35, 40]. Developing such models without considering the external shocks may result in an underestimated failure probability, deceptive reliability estimations and, consequently, misleading maintenance decisions. In this paper, we develop a numerical maintenance optimization model for continuously monitored systems that are subject to both gradual degradation and stochastic shocks caused by external factors based on a Wiener process. In the model, the random shocks can happen throughout the whole deterioration process with different stochastic magnitudes. The magnitude can be large enough to result in a direct

failure, where the system goes beyond the failure threshold immediately or it can be smaller and simply increase the degradation level by a random extent. Comparing our results with the Wiener process shows that the combination of shocks and gradual degradation provides a more practical and realistic reliability estimation and, thus, more efficient maintenance decisions for systems with Wiener-based degradation behavior.

Another assumption often made in maintenance models for continuously monitored systems subject to shocks is the negligible lead time before maintenance implementation. In some research works, the authors often focus on multi-component systems with dependent failure processes, while they assume that the lead time duration is too short and can be neglected [6,42]. However, some applications such as offshore wind farms and power plant facilities located in remote areas often experience large production loss due to prolonged lead-time delays while procuring critical spares [7,34]. In this paper, we also incorporate the maintenance lead time into our model and account for the probability of system failures occurring within this period.

### 5. Conclusions and further work

This paper proposes a numerical framework to find the optimal maintenance threshold for single-component continuously monitored systems that are exposed to both gradual degradation and external shocks with stochastic magnitudes, in the presence of a deterministic

### Algorithm 3

Extracting shocks from run-to-failure datasets.

```

for t = 1 do
 $I_t = Y_t$ 
end for
for t = 2 to Number of samples do
Calculate the degradation increments by  $I_t = Y_t - Y_{t-1}$ 
if  $I_t > 2 \times \sigma_1$ 
The increment is assumed to be a shock which arises from external events
else
The increment is assumed to be a result of gradual degradation (aging)
end if
end for
    
```

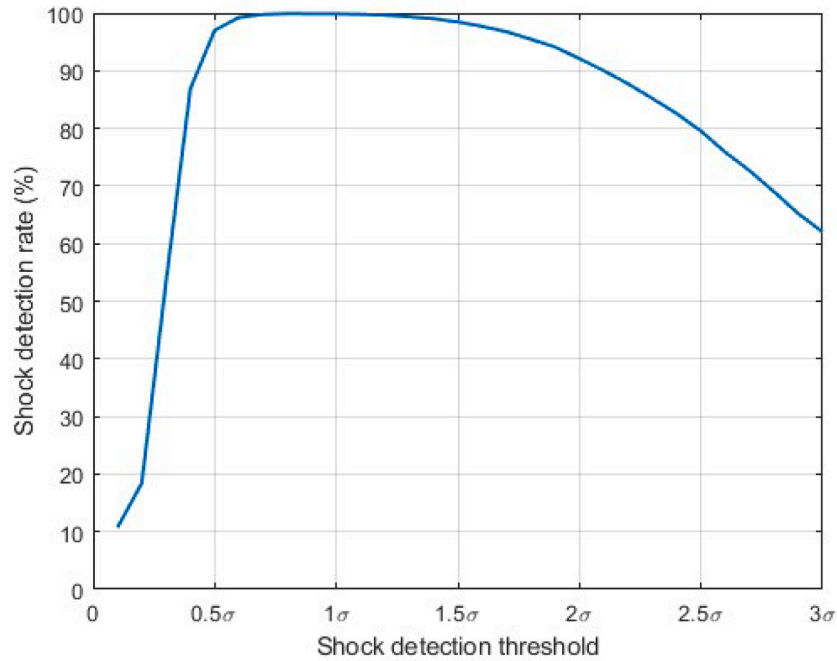


Fig. 12. Shock detection rate versus threshold,  $\sigma$  is the standard deviation of the degradation increments.

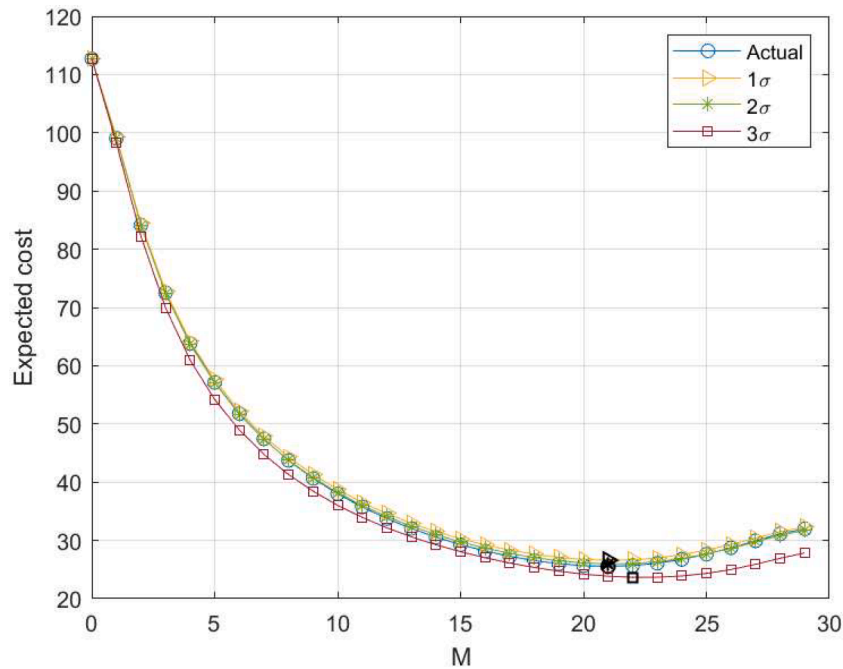


Fig. 13. Impact of shock detection threshold on expected cost.

lead time. The shocks can be both fatal and non-fatal, depending on the health condition of the system. The probability of system failure due to a fatal shock increases as the system approaches the failure threshold. The numerical solution does not resort to MCS, but it was compared with MCS to validate the proposed model. The result shows that our numerical approach can efficiently and accurately find the optimal maintenance threshold. The advantages of the proposed model have been highlighted in comparison with the Wiener process, and it was demonstrated that the shock model is more beneficial and realistic for risk analysis, decision-making, and maintenance optimization by incorporating the shocks or extreme events. The model is employed on both a

numerical example and a real-life bearings dataset to show its applicability. While the model is initially proposed for systems characterized by the Wiener process, it can be slightly modified and adapted to systems that exhibit a geometric Brownian motion (GBM) by considering the dependency between degradation increments. This flexibility makes the model more applicable to a wider range of systems with different degradation behaviors.

For further work, it would be valuable to study the uncertainty of model parameters to increase the model robustness and improve future decision-making. One of the possible approaches to consider uncertainty is to perform a sensitivity analysis to figure out how changing each



individual parameter affects the total expected cost. The result of such analysis can help the operators make decisions that are more considerate of the parameters' uncertainty. Another approach to reduce uncertainty is to update the key parameters of the model throughout the degradation process once more degradation observation is available. The key parameters include parameters of the Wiener process and shock process, failure threshold, cost values, and lead time, which can be treated as stochastic variables instead of deterministic. In addition, shocks arise from different sources in practice. Some are caused by dynamic environmental conditions such as seasonal weather variation, and some others by cascading failures due to other components that have an interaction with the system of interest. Thus, the intensity rate of random shocks can be treated as a stochastic variable and can vary through the system degradation.

Moreover, in our proposed model, there is only one objective function, which is the total expected cost. Another interesting point to consider is to integrate human factors in the model and further investigate how risk perception and cognitive biases of decision-makers can influence the maintenance threshold. In real-world applications, decision-makers may not only consider costs, but also non-monetary factors such as environmental damage and safety concerns. Another potential direction of further work is to take a system-level approach, where the interdependencies and interactions between several components are taken into account. This makes the model more realistic and applicable for complex industrial systems.

#### CRedit authorship contribution statement

**Bahareh Tajiani:** Writing – original draft, Visualization, Validation, Methodology, Investigation, Formal analysis, Data curation, Conceptualization. **Jørn Vatn:** Writing – review & editing, Supervision, Methodology, Conceptualization. **Masoud Naseri:** Writing – review & editing, Conceptualization.

#### Declaration of competing interest

The authors declare that they have no conflict of interest in connection with the submitted work.

#### Data availability

Data will be made available on request.

#### References

- [1] Ardourel V, Jebeile J. Numerical instability and dynamical systems. *Eur J Philos Sci* 2021;11(2):1–21. [10.1007/S13194-021-00372-7/FIGURES/6](https://doi.org/10.1007/S13194-021-00372-7/FIGURES/6).
- [2] Bérenguer C, et al. Maintenance policy for a continuously monitored deteriorating system. *Probab Eng Inf Sci* 2003;17(2):235–50. <https://doi.org/10.1017/S0269964803172063>.
- [3] Bozbulut, A.R. and Eryilmaz, S. (2018) 'Generalized extreme shock models and their applications', *10.1080/03610918.2018.1476699*, 49(1), pp. 110–20. [10.1080/03610918.2018.1476699](https://doi.org/10.1080/03610918.2018.1476699).
- [4] Byon E, Ntaimo L, Ding Y. Optimal maintenance strategies for wind turbine systems under stochastic weather conditions. *IEEE Trans Reliab* 2010;59(2): 393–404. <https://doi.org/10.1109/TR.2010.2046804>.
- [5] Caballé NC, et al. A condition-based maintenance of a dependent degradation-threshold-shock model in a system with multiple degradation processes. *Reliab Eng Syst Saf* 2015;134:98–109. <https://doi.org/10.1016/J.RESS.2014.09.024>.
- [6] Castro, I.T., Caballé, N.C. and Pérez, C.J. (2013) 'A condition-based maintenance for a system subject to multiple degradation processes and external shocks', *10.1080/00207721.2013.828796*, 46(9), pp. 1692–704. [10.1080/00207721.2013.828796](https://doi.org/10.1080/00207721.2013.828796).
- [7] Dawid R, McMillan D, Revie M. Review of Markov models for maintenance optimization in the context of offshore wind. In: *Proceedings of the annual conference of the prognostics and health management society*; 2015.
- [8] Deloux E, Castanier B, Bérenguer C. Predictive maintenance policy for a gradually deteriorating system subject to stress. *Reliab Eng Syst Saf* 2009;94(2):418–31. <https://doi.org/10.1016/J.RESS.2008.04.002>.
- [9] Dong W, et al. Reliability modelling for multi-component systems subject to stochastic deterioration and generalized cumulative shock damages. *Reliab Eng Syst Saf* 2021;205:107260. <https://doi.org/10.1016/J.RESS.2020.107260>.
- [10] Duan C, et al. An adaptive reliability-based maintenance policy for mechanical systems under variable environments. *Reliab Eng Syst Saf* 2023;238:109396. <https://doi.org/10.1016/J.RESS.2023.109396>.
- [11] Dui H, Zhang H, Wu S. Optimisation of maintenance policies for a deteriorating multi-component system under external shocks. *Reliab Eng Syst Saf* 2023;238: 109415. <https://doi.org/10.1016/J.RESS.2023.109415>.
- [12] Elwany, A.H. et al. (2011) 'Structured replacement policies for components with complex degradation processes and dedicated sensors', *10.1287/opre.1110.0912*, 59(3), pp. 684–95. [10.1287/opre.1110.0912](https://doi.org/10.1287/opre.1110.0912).
- [13] Gan S, Hu H, Coit DW. Maintenance optimization considering the mutual dependence of the environment and system with decreasing effects of imperfect maintenance. *Reliab Eng Syst Saf* 2023;235:109202. <https://doi.org/10.1016/J.RESS.2023.109202>.
- [14] Godoy DR, Pascual R, Knights P. Critical spare parts ordering decisions using conditional reliability and stochastic lead time. *Reliab Eng Syst Saf* 2013;119: 199–206. <https://doi.org/10.1016/J.RESS.2013.05.026>.
- [15] Grall A, Bérenguer C, Dieulle L. A condition-based maintenance policy for stochastically deteriorating systems. *Reliab Eng Syst Saf* 2002;76(2):167–80. [https://doi.org/10.1016/S0951-8320\(01\)00148-X](https://doi.org/10.1016/S0951-8320(01)00148-X).
- [16] Hao S, Yang J. Dependent competing failure modeling for the gil subject to partial discharge and air leakage with random degradation initiation time. *IEEE Trans Reliab* 2019;68(3):1070–9. <https://doi.org/10.1109/TR.2018.2875819>.
- [17] He J, Cheng Z, Guo B. Anomaly detection in telemetry data using a jointly optimal one-class support vector machine with dictionary learning. *Reliab Eng Syst Saf* 2023;242:109717. <https://doi.org/10.1016/J.RESS.2023.109717>.
- [18] Hua M, Peskin CS. An analysis of the numerical stability of the immersed boundary method. *J Comput Phys* 2022;467:111435. <https://doi.org/10.1016/j.jcp.2022.111435>.
- [19] Huang X, et al. Reliability analysis of coherent systems subject to internal failures and external shocks. *Reliab Eng Syst Saf* 2019;181:75–83. <https://doi.org/10.1016/J.RESS.2018.09.003>.
- [20] Jiang R. Optimization of alarm threshold and sequential inspection scheme. *Reliab Eng Syst Saf* 2010;95(3):208–15. <https://doi.org/10.1016/J.RESS.2009.09.012>.
- [21] Juybari MN, Hamadani AZ, Ardakan MA. Availability analysis and cost optimization of a repairable system with a mix of active and warm-standby components in a shock environment. *Reliab Eng Syst Saf* 2023;237:109375. <https://doi.org/10.1016/J.RESS.2023.109375>.
- [22] Li W, Pham H. A Condition-Based Inspection-Maintenance Model Based on Geometric Sequences for Systems With a Degradation Process and Random Shocks. *Life Cycle Reliab. Saf. Eng.* 2012;1(1):24–36. Available at, [www.sresa.org.in/SRESA-Journal-Issue-1-3.pdf](http://www.sresa.org.in/SRESA-Journal-Issue-1-3.pdf).
- [23] Liang Q, Peng C, Li X. A multi-state Semi-Markov model for nuclear power plants piping systems subject to fatigue damage and random shocks under dynamic environments. *Int J Fatigue* 2023;168:107448. [10.1016/J.IJFATIGUE.2022.107448](https://doi.org/10.1016/J.IJFATIGUE.2022.107448).
- [24] Liang Q, Yang Y, Peng C. A reliability model for systems subject to mutually dependent degradation processes and random shocks under dynamic environments. *Reliab Eng Syst Saf* 2023;234:109165. <https://doi.org/10.1016/J.RESS.2023.109165>.
- [25] Lin YH, Li YF, Zio E. Reliability assessment of systems subject to dependent degradation processes and random shocks. *IIE Trans. Inst. Indus. Eng.* 2016;48(11): 1072–85. <https://doi.org/10.1080/0740817X.2016.1190481>.
- [26] Lin YH, Li YF, Zio E. A comparison between Monte Carlo simulation and finite-volume scheme for reliability assessment of multi-state physics systems. *Reliab Eng Syst Saf* 2018;174:1–11. <https://doi.org/10.1016/J.RESS.2018.01.008>.
- [27] Liu B, et al. An imperfect maintenance policy for mission-oriented systems subject to degradation and external shocks. *Comput Ind Eng* 2016;102:21–32. <https://doi.org/10.1016/J.CIE.2016.10.008>.
- [28] Oakley JL, Wilson KJ, Philipson P. A condition-based maintenance policy for continuously monitored multi-component systems with economic and stochastic dependence. *Reliab Eng Syst Saf* 2022;222:108321. <https://doi.org/10.1016/J.RESS.2022.108321>.
- [29] Pedersen TI, Liu X, Vatn J. Maintenance optimization of a system subject to two-stage degradation, hard failure, and imperfect repair. *Reliab Eng Syst Saf* 2023; 237:109313. <https://doi.org/10.1016/J.RESS.2023.109313>.
- [30] Pedersen TI, Vatn J. Optimizing a condition-based maintenance policy by taking the preferences of a risk-averse decision maker into account. *Reliab Eng Syst Saf* 2022;228:108775. <https://doi.org/10.1016/J.RESS.2022.108775>.
- [31] Sarada Y, Shenbagam R. Optimization of a repairable deteriorating system subject to random threshold failure using preventive repair and stochastic lead time. *Reliab Eng Syst Saf* 2021;205:107229. <https://doi.org/10.1016/J.RESS.2020.107229>.
- [32] Sun F, et al. Reliability analysis for a system experiencing dependent degradation processes and random shocks based on a nonlinear Wiener process model. *Reliab Eng Syst Saf* 2021;215:107906. <https://doi.org/10.1016/J.RESS.2021.107906>.
- [33] Tajiani B, Vatn J. Adaptive remaining useful life prediction framework with stochastic failure threshold for experimental bearings with different lifetimes under contaminated condition. *Int. J. Syst. Assuran. Eng. Manag* 2023;1:1–22. <https://doi.org/10.1007/S13198-023-01979-0>.
- [34] Wakiru J, et al. Maintenance optimization: application of remanufacturing and repair strategies. *Procedia CIRP* 2018;69:899–904. <https://doi.org/10.1016/J.PROCIR.2017.11.008>.

- [35] Wang HK, et al. Condition-based maintenance with scheduling threshold and maintenance threshold. *IEEE Trans Reliab* 2016;65(2):513–24. <https://doi.org/10.1109/TR.2015.2487578>.
- [36] Wang J, Bai G, Zhang L. Modeling the interdependency between natural degradation process and random shocks. *Comput. Indus. Eng.* 2020;145. <https://doi.org/10.1016/J.CIE.2020.106551>.
- [37] Wang S, et al. Joint optimization of multi-stage component reassignment and preventive maintenance for balanced systems considering imperfect maintenance. *Reliab Eng Syst Saf* 2023;237:109367. <https://doi.org/10.1016/J.RESS.2023.109367>.
- [38] Wang W, Chen X. Piecewise deterministic Markov process for condition-based imperfect maintenance models. *Reliab Eng Syst Saf* 2023;236:109271. <https://doi.org/10.1016/J.RESS.2023.109271>.
- [39] Wang X, et al. Mixed shock model for multi-state weighted k-out-of-n: f systems with degraded resistance against shocks. *Reliab Eng Syst Saf* 2022;217:108098. <https://doi.org/10.1016/J.RESS.2021.108098>.
- [40] Wang Z, et al. A prognostics-based spare part ordering and system replacement policy for a deteriorating system subjected to a random lead time. *Int J Prod Res* 2015;53:4511–27. <https://doi.org/10.1080/00207543.2014.988892>.
- [41] Yang L, et al. A preventive maintenance policy based on dependent two-stage deterioration and external shocks. *Reliab Eng Syst Saf* 2017;160:201–11. <https://doi.org/10.1016/J.RESS.2016.12.008>.
- [42] Yousefi N, et al. Optimization of on-condition thresholds for a system of degrading components with competing dependent failure processes. *Reliab Eng Syst Saf* 2019;192:106547. <https://doi.org/10.1016/J.RESS.2019.106547>.
- [43] Zhang N, et al. Reliability and maintenance analysis of a degradation-threshold-shock model for a system in a dynamic environment. *Appl Math Model* 2021;91:549–62. <https://doi.org/10.1016/J.APM.2020.09.047>.
- [44] Zhang N, et al. Joint optimization of condition-based maintenance and condition-based production of a single equipment considering random yield and maintenance delay. *Reliab Eng Syst Saf* 2024;241:109694. <https://doi.org/10.1016/J.RESS.2023.109694>.
- [45] Zhang Z, et al. Degradation data analysis and remaining useful life estimation: a review on Wiener-process-based methods. *Eur J Oper Res* 2018;271:775–96. <https://doi.org/10.1016/j.ejor.2018.02.033>.
- [46] Zhao X, et al. Optimal condition-based maintenance policy with delay for systems subject to competing failures under continuous monitoring. *Comput. Indus. Eng.* 2018;124:535–44. <https://doi.org/10.1016/J.CIE.2018.08.006>.